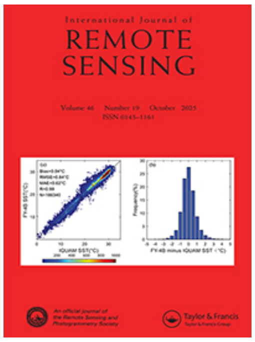

International Journal of Remote Sensing

ISSN: 0143-1161 (Print) 1366-5901 (Online) Journal homepage: www.tandfonline.com/journals/tres20

Synergistic use of Sentinel-1 and Sentinel-2 data for Fall Armyworm infestation detection and mapping in maize croplands

Tatenda Dzurume, Roshanak Darvishzadeh, Timothy Dube, T.S Amjath Babu, Mutasim Billah, Syed Nurul Alam, Mustafa Kamal, Md. Harun-Or-Rashid, Badal Chandra Biswas, Md. Ashraf Uddin, Md. Abdul Muyeed, Md. Mostafizur Rahman Shah, Timothy J. Krupnik & Andrew Nelson

To cite this article: Tatenda Dzurume, Roshanak Darvishzadeh, Timothy Dube, T.S Amjath Babu, Mutasim Billah, Syed Nurul Alam, Mustafa Kamal, Md. Harun-Or-Rashid, Badal Chandra Biswas, Md. Ashraf Uddin, Md. Abdul Muyeed, Md. Mostafizur Rahman Shah, Timothy J. Krupnik & Andrew Nelson (2025) Synergistic use of Sentinel-1 and Sentinel-2 data for Fall Armyworm infestation detection and mapping in maize croplands, International Journal of Remote Sensing, 46:19, 7044-7076, DOI: 10.1080/01431161.2025.2546155

To link to this article: https://doi.org/10.1080/01431161.2025.2546155

INTERNATIONAL JOURNAL OF REMOTE SENSING
2025, VOL. 46, NO. 19, 7044–7076
https://doi.org/10.1080/01431161.2025.2546155

Synergistic use of Sentinel-1 and Sentinel-2 data for Fall Armyworm infestation detection and mapping in maize croplands

Tatenda Dzurume [a,b], Roshanak Darvishzadeh [a], Timothy Dube [b], T. S Amjath Babu [c], Mutasim Billah [c], Syed Nurul Alam[c], Mustafa Kamal [c], Md. Harun-Or-Rashid [c], Badal Chandra Biswas[d], Md. Ashraf Uddin[d], Md. Abdul Muyeed[d], Md. Mostafizur Rahman Shah [e], Timothy J. Krupnik [c] and Andrew Nelson [a]

[a]Department of Natural Resources, Faculty of Geo-Information Science and Earth Observation, University of Twente, Enschede, the Netherlands; [b]Institute for Water Studies, University of the Western Cape, Bellville, South Africa; [c]Sustainable Agrifood Systems Program, International Maize and Wheat Improvement Center (CIMMYT), Dhaka, Bangladesh; [d]Department of Agricultural Extension, Ministry of Agriculture, Dhaka, Bangladesh; [e]Bangladesh Wheat and Maize Research Institute, Dinajpur, Bangladesh

ABSTRACT

Fall Armyworm (FAW) is a widespread invasive pest in maize crops. This study aimed at detecting and mapping FAW infestations in maize fields across Bangladesh, using freely available Sentinel-1 and Sentinel-2 data. Field observations were conducted during the 2019–2020 maize growing season in 579 maize fields across six administrative divisions of Bangladesh. The study covered both infested and non-infested sites across four crop growth phases, namely vegetative phases 9 (V9) and 12 (V12), as well as the silking and maturing phases. Synthetic Aperture Radar backscatter values, spectral reflectance profiles, and eight vegetation indices were extracted from the Sentinel data and analysed using non-parametric statistical tests to identify differences between infested and non-infested fields. Machine learning models, specifically Random Forest - and Support Vector Machine, were then used to classify infestation severity based on five model input data combinations: (i) Sentinel-1, (ii) Sentinel-2, (iii) Sentinel-2 with vegetation indices, (iv) Sentinel-1 and Sentinel-2, and (v) Sentinel-1, Sentinel-2, and vegetation indices. The results indicated that infested maize fields exhibited reduced near-infrared reflectance and distinct backscatter patterns in σ_{VH}^{o}, with notable variations at silking and maturity phases. The red edge (740 nm), near-infrared (865 nm) and short-wave infrared (1610–2190 nm) bands were particularly effective in distinguishing infestation levels across all growing phases. Among

ARTICLE HISTORY
Received 6 April 2025
Accepted 5 August 2025

KEYWORDS
Bangladesh; change detection; Fall Armyworm infestation; optical; SAR; structural changes

CONTACT Tatenda Dzurume t.dzurume@utwente.nl/3459290@myuwc.ac.za Department of Natural Resources, Faculty of Geo-Information Science and Earth Observation, University of Twente, Hallenweg 8, PO Box 217, Enschede 7500 AE, the Netherlands

Supplemental data for this article can be accessed online at https://doi.org/10.1080/01431161.2025.2546155

the studied vegetation indices, the Normalized Difference Vegetation Index , Modified Chlorophyll Absorption in Reflectance Index, Red Edge Simple Ratio, and Modified Simple Ratio - were identified as the most significant indicators for discriminating between non-infested and infested maize classes at all growing phases. RF achieved 94–96% accuracy (96% in V9) versus SVM's 78–80% using only Sentinel-1 data. Multi-source (Sentinel-1, Sentinel-2 and Vegetation Indices) integration improved both models in most cases. These results underscore the potential of integrating multi-source remote sensing data for scalable and accurate pest detection. Freely available Sentinel data is a valuable source of information for early pest detection and management aiding policymakers in identifying high-risk areas, implementing timely interventions, and promoting sustainable pest management strategies to protect maize production and reduce economic losses.

1. Introduction

Maize (*Zea mays L.*) is the most widely cultivated cereal crop worldwide (Galani et al. 2022). However, its production is challenged by various factors, including climate change, soil salinity, poor soil structure as well as diseases and pests (Chinwada et al., 2021; Fernández and Hoeft 2009; Brouder and Volenec 2008). Globally, yield losses due to diseases and pests are estimated between 19.5% and 41.1% (Savary et al. 2019). Pest-infested maize is likely to experience reduced photosynthetic carbon fixation, leading to decreased crop growth and productivity (Tanyi et al. 2020). One of the most significant threats to global maize production is the rapid spread of the Fall Armyworm (FAW), *Spodoptera frugiperda* (J.E. Smith) (Lepidoptera: Noctuidae). Among the 38 pests and pathogens studied in maize, FAW ranked among the top six, causing global maize losses exceeding 1% (Savary et al. 2019). FAW poses a severe risk to maize production, particularly in tropical and subtropical regions. According to Senay et al. (2022) approximately half of the world's maize growing areas are vulnerable to year around FAW infestations. In Africa, nearly 92% of maize cultivation zones support continuous FAW growth, leading to estimated annual yield losses of up to US $9.4 billion (Eschen et al. 2021). The invasion of FAW in Africa and the Asia-Pacific region has had devastating effects. First reported in Africa in 2016 (Day et al. 2017), FAW has since spread to at least 44 African countries (Ishengoma et al. 2021; Kassie et al. 2020), threatening food security and livelihoods (Durocher-Granger et al. 2024). In some maize-dependent regions, FAW infestations have led to yield losses ranging from 21% to 54%, resulting in economic losses between US $74.5 million and US $185.5 million annually (Tabu et al. 2024). In Asia, FAW infestations have been reported in 19 countries, including India, Nepal, Sri Lanka, Pakistan, Thailand, Vietnam, and Bangladesh (Attaluri et al. 2022). While FAW is highly adaptable and polyphagous pest, capable of feeding various crops, including sorghum, sugarcane, wheat and rice, maize remains the most affected in Africa (Nwanze et al. 2021; Prasanna et al. 2021; Montezano et al. 2018).

FAW resembles both the African armyworm and the corn earworm. It is identifiable by distinct morphological features including: (a) a white inverted 'Y' mark on the front of the dark head; (b) a brown head with dark honeycomb marks; and (c) four dark spots arranged

Figure 1. (a) The most common features used for the identification of FAW (*source https://www.corteva.com.au/agronomy-hub/faw.html*.;accessed on 10 August 2024) (b) Structural damage caused by FAW on maize crops. (*source* https://www.farmersweekly.co.za/crops/field-crops/researchers-advance-in-fight-to-control-fall-armyworm/attachment/fall-armyworm-larvae-can-cause-damage-to-maize/.; accessed on 10 August 2024).

in a square on the top of the eighth abdominal segment (Matova et al. 2020), as highlighted in Figure 1(a). FAW has been recognized as the second most damaging agricultural pest (Kumela et al. 2019). FAW invasions have affected trade, income, and food security due to reductions in maize production. Additionally, FAW invasions increase health risks due to insecticide exposure and disrupt the performance of businesses along the maize value chain, including maize input suppliers and contributors to the livestock feed sector (Abro et al. 2021). Infestation by FAW also incurs additional costs due to insecticide use and labour needed to control the pest (Abro et al. 2021).

Major challenges facing farmers due to FAW include crop loss, increased costs of management, difficulty in controlling FAW, insecticide resistance, uneven growth and maturity, and unfamiliar crop damage. The noticeable effects of FAW infestation include leaf and stem damage characterized by holes and ragged edges, disruption of canopy integrity and structure (as shown in Figure 1(b)), and uncertainty in crop outcomes. FAW is expected to continue causing maize crop losses in Africa, Asia-Pacific and Oceania likely due to increase in temperature, continuous maize cultivation and diverse host crops. However, losses vary from place to place depending on climate suitability for growth and development as well as adopted crop and pest management practices.

Different approaches (Prasannaet et al. 2021; Lamsal et al. 2020; Sisay et al. 2019) have been used to detect and characterize crop injuries caused by FAW, often relying on traditional methods such as field surveys. While these methods are essential for data validation, they are typically time-consuming and resource-intensive (Prabhakar et al. 2022; Zhang et al. 2019), making it difficult to (rapidly) assess infestations across broad spatial scales. Consequently, there is an urgent need for innovative, and scalable solutions.

Earth observation data (EO) offers a promising spatial explicit complementary approach to pest detection, enabling faster detection, efficient monitoring, and targeted responses to combat this invasive pest/diseases and protect essential food production. EO can complement surveys by measuring the extent of damage caused by pest through detecting changes in the crop canopy (Isip et al. 2020). Recent developments in optical and SAR EO technology have made it possible to differentiate between non-infested and infested crops. The use of EO for detecting crop pests and diseases, such as FAW infestation, is based on the assumption that stresses (e.g. such as uneven growth, irregular maturity, and disrupted canopy structure), induced by these factors interfere with photosynthesis and the light absorption, hence altering the reflectance characteristics of crops (Prabhakar et al. 2013).

Studies have used hyperspectral and multispectral data to understand the impacts of pests and diseases on crops (see Supplementary Table S1). Specifically, Filho et al. (2022) explored hyperspectral remote sensing to detect reflectance changes in soybean caused by stinkbug and caterpillar infestations. Greenhouse experiments with varying insect densities showed that stinkbugs had little effect on reflectance, while caterpillars caused detectable changes. A deep-learning model accurately classified infestation levels, demonstrating hyperspectral sensing as a promising tool for early caterpillar detection in soybean crops. Dutta et al. (2024) developed a two-step methodology using hyperspectral imaging for early detection of wilt disease in pigeonpea (*Cajanus cajan*), caused by *Fusarium udum* in India. By integrating spectral indices and endmember analysis from ASI-PRISMA, DLR DESIS, and EnMAP datasets, they established a disease-specific spectral index ($\leq$0.55) and stress threshold ($\geq$3) for identifying infected crops 2–3 weeks earlier than conventional methods. In a study conducted in Brazil, Furuya et al. (2021), used hyperspectral imaging combined with advanced machine learning techniques to achieve early detection of insect herbivory damage in maize crops. The researchers collected leaf spectral data over eight consecutive days using a FieldSpec 3.0 Spectroradiometer from three groups of crops: undamaged controls, those damaged by *Spodoptera frugiperda*, and those damaged by *Dichelops meiacanthus*. Additionally, the study revealed that the near-infrared spectral region was the most effective in differentiating between healthy and insect-damaged maize.

Multispectral images are widely used in agricultural studies to obtain various crop parameters and for other applications, as demonstrated in studies by Prabhakar et al. (2022) and Balla et al. (2019). Further, studies have shown that spectral data from the red, red edge and near-infrared regions is particularly suited for detecting pests and disease related crop injuries (Tussupov et al. 2024; Xulu et al. 2024; Meng et al. 2020; Adelabu, et al., 2014; Mahlein et al., 2010; Franke and Menz 2007). The reflectance from the red edge region is sensitive to variation of chlorophyll which is an indicator of crop functioning, health and potential stress caused by biotic and abiotic stress (Chauhan et al. 2019).

Adverse weather conditions and cloud cover can significantly impede the effectiveness of optical sensors in detecting diseases and pest damage (Kaushik et al. 2021). Synthetic Aperture Radar (SAR), an active microwave sensor, overcomes these limitations with its penetration capability, providing a more reliable approach for detecting diseases and pest damage. Vertical-Horizontal (σ_{VH}^{o}) and Vertical-Vertical (σ_{VV}^{o}) polarizations obtained from SAR sensors provide critical information about crop structure and condition (Ma et al. 2024; Chauhan et al. 2020). σ_{VH}^{o} is typically more sensitive to changes in vegetation structure, such as canopy density and leaf orientation, making it effective for detecting pest damage or disease. On the other hand, σ_{VV}^{o} primarily captures surface scattering and is influenced by factors like soil moisture and overall crop biomass.

Machine learning classification algorithms (ML) such as Support Vector Machine and Random Forest have gained popularity for analysing and classifying EO-based information on crop cover and its condition. These ML classifiers are widely used across various disciplines and ecosystems due to their ability to handle complex datasets, discriminate between subtle differences in crop types, and assess crop health with high accuracy. The Support Vector Machine can accommodate both high dimensionality and limited training sample sizes and, on the other hand, Random Forest has the ability to learn both simple and complex classification functions (Zhang et al. 2016; Breiman, 2001) .

Recent advancements in optical and SAR data integration, coupled with improvements in ML algorithms have enabled EO-based assessments of diseases and pest damage on field crops. Das et al. (2024) assessed forest health, considering both biotic and abiotic stressors, using Sentinel-1 and Sentinel-2 data to develop regression models for leaf area index in United States of America. The Random Forest classifier out-performed the Support Vector Machine classifier, with high prediction accuracy ($R^2 > 0.76$). Prabhakar et al. (2022) assessed FAW damage on sorghum using Sentinel 2 data and ground observations in farm fields of southern India. FAW infestation reduced the leaf area index by 50%, biomass by 33%, and grain yield by 52%, with the panicle initiation phase experiencing the highest yield loss. In another study by Dhau et al. (2021), the use of Sentinel 2 data for detecting and mapping Maize Streak Virus was studied at smallholder Ofcolaco farms of South Africa. The results showed high accuracy using Random Forest classification in detecting infected maize, with an overall accuracy of 89% and Kappa of 0.84 when combining spectral bands with vegetation indices. Ainunnisa and Haerani (2023) studied pest and disease infections in rice fields using Sentinel-2 satellite imagery in Indonesia. Two vegetation indices (Normalized Difference Vegetation Index and the Normalized Difference Red Edge index) were analysed through spatial analysis and simple linear regression to assess their relationship with rice productivity. Results indicated that both indices had low values corresponded to pest and disease infections, such as rats, rice leaf folders, borers, and blasts, which reduced rice production.

Previous studies (Veloso et al., 2017; Bouman and van Kasteren 1990) have shown that SAR backscatter is dominated by surface scattering from soil due to small maize crops, especially during growth phases vegetative phase 3 to vegetative phase 7. Prior use of Sentinel 2 data to examine growth phases V3-V8 for FAW infestation has provided valuable insights into spectral reflectance patterns under varying levels of FAW infestation, supporting a more focused examination of critical growth phases in this study (Dzurume et al. 2025).

The rapid spread of FAW presents a serious challenge to crop production, especially in regions with limited resources for traditional monitoring. While previous studies have explored remote sensing for pest detection, many rely on either optical or radar data alone or apply conventional classification techniques with limited adaptability. In this study, we propose an innovative framework that integrates Sentinel-1 (SAR) and Sentinel-2 (optical) data to capitalize on the complementary strengths of both sensors. This fusion enhances the monitoring capacity under various weather and illumination conditions. We further use RF and SVM classifiers to improve detection accuracy and model robustness. This approach emphasizes feature-level fusion and texture/spectral feature extraction to better characterize FAW-affected areas. This multi-source, multi-method approach provides a novel contribution to remote sensing-based FAW monitoring, offering a more resilient and transferable solution compared to existing methods.

The combination of Sentinel-1 and Sentinel-2 offers key advantage, including all-weather capability, frequent revisits, and efficient processing. Sentinel-1's SAR ensures continuous monitoring, unaffected by clouds, while Sentinel-2 provides high-resolution optical imagery for crop health analysis. By integrating structural information from Sentinel-1 with spectral information from Sentinel-2, users gain a cost-effective, practical solution for large-scale, real-time applications like agriculture. The reviewed literature indicates that no study has combined optical and SAR satellite data to discriminate FAW infested maize fields across the range of growing phases where FAW-related damage occurs. Therefore, this study (i) identified the key SAR and reflectance data needed to distinguish between infested and non-infested maize across four phases and (ii) examined how various combinations of SAR and optical data from Sentinel-1 and Sentinel-2, when paired with supervised machine learning algorithms, could effectively differentiate FAW-infested maize from non-infested maize at different crop growth phases. The widespread occurrence of FAW and the global availability of EO data (Sentinel 1 and Sentinel 2) that can detect structural and physiological changes in field crops due to pest damage suggests that our study is a relevant and valuable contribution to the literature.

2. Materials and methods

Figure 2 shows the workflow in the study. Each step is explained in the following subsections.

2.1. Study area

The study was conducted across six divisions of Bangladesh (Figure 3). Maize is the country's second most important cereal crop. (Prasanna et al. 2021). In Bangladesh, maize is both consumed directly and used as feed for livestock and poultry. Maize is generally grown in both the Kharif (March–June) and Rabi (November–May) seasons in fields ranging from 1 to 3 ha (Figure 4). It is primarily grown during the Kharif season in the

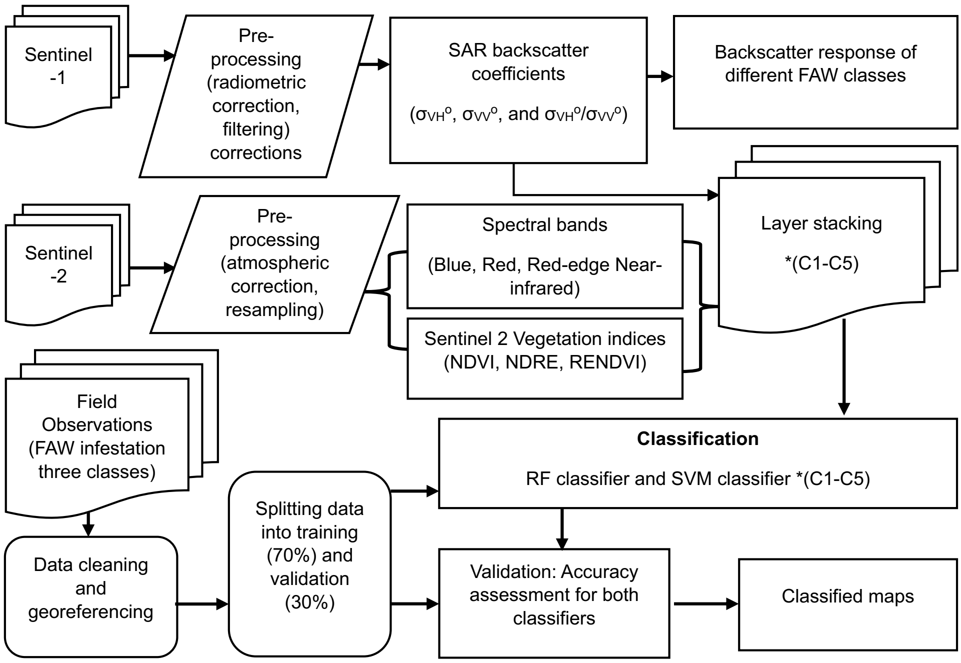

Figure 2. Flowchart shows the steps that were followed in this study. *C1–C5 refers to the five different input datasets (combinations) used in this study.

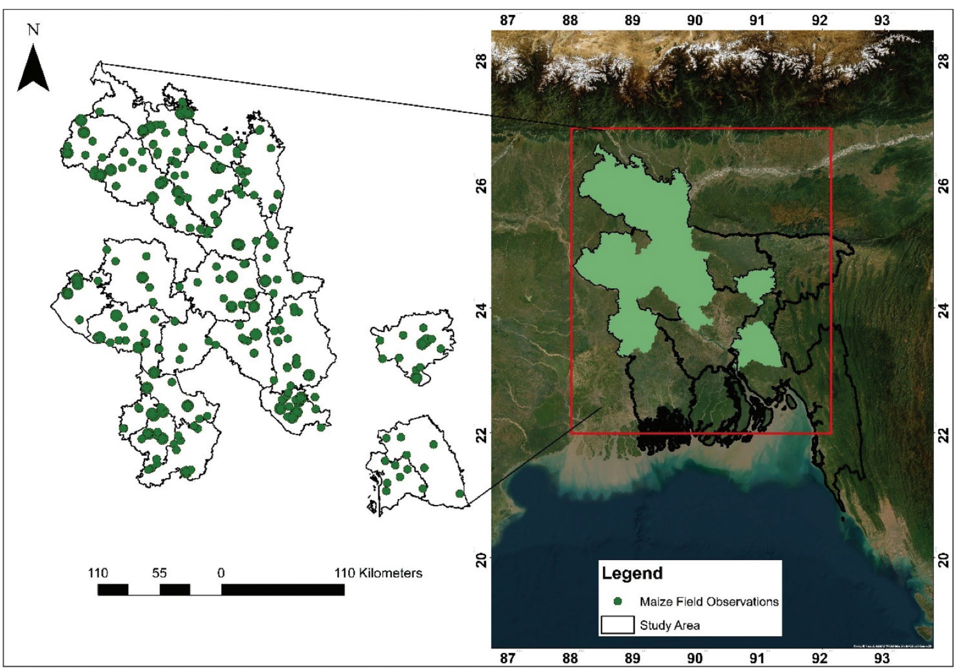

Figure 3. The study area and the locations of the 579 fields in the six divisions for the four selected maize growth phases.

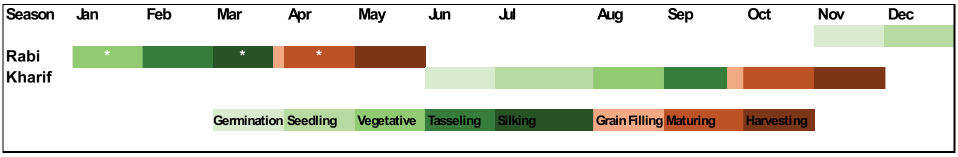

Figure 4. Maize-growing seasons in Bangladesh: Rabi and Kharif. This study examines four specific growth phases of maize cultivated during the Rabi season (denoted by an asterisk *).

central and eastern districts and the Rabi season in the northern and western districts. Despite significant growth in maize production and cultivation (Khatun et al. 2024), farmers have recently faced numerous challenges, including unstable weather, high maize seed prices, market instability, and pest attacks, such as FAW (Islam and Hoshain 2022). FAW was first detected in Bangladesh in November 2018 and subsequently spread across 22 districts before being formally identified in May 2019 (Khatun et al. 2024). High temperatures in Bangladesh provide an ideal environment for FAW to thrive.

2.2. Field observation data

Field data collection was carried out between the growing season of December 2019 to May 2020. The field campaign was conducted in six divisions of Bangladesh (Chattogram, Dhaka, Khulna, Rajshahi, Rangpur, and Mymensingh) by CIMMYT Bangladesh. The field data observers were trained by the Department of Agricultural Extension (DAE) in Bangladesh to follow the scouting method for data collection. However, it is important to note that a potential limitation is that the field data observers were not constantly monitored throughout the duration of the data collection. The same maize fields were visited during the campaign at different growth phases. Approximately 7,000 maize field observations were collected across 579 fields through weekly scouting and included the following variables: (*i-iv*) division, district, upazila, union; (*v*) trap tag; (*vi*) longitude and latitude; (*vii*) submission time; (*viii*) phase; (*ix*) count of moths; and (*x*) infestation of cobs.

The field observation period spans from vegetative emergence to maturity phases. To focus on key growth phases relevant to the study, only field observations from the V9, V12, silking, and maturing phases were retained. As the crop grows and canopy cover increases, surface scattering from the soil decreases. Therefore, based on the outlined reasons and for the purpose of this study, we focus on vegetative phase 9 (V9), vegetative phase 12 (V12), silking and maturing phases. Focusing on the V9, V12, silking, and maturing phases allows the capture of key growth phases with distinct spectral and SAR signatures that are crucial for assessing crop health and yield potential. The selected phases align well with crucial agronomic decisions, such as fertilizer application, irrigation, and pest management, which are often concentrated in these periods.

Data cleaning excluded observations from growth phases outside the specified range and any coordinates outside the field boundaries based on visual interpretation with Google Earth images (https://earth.google.com). This reduced the dataset to 1,275 field observations across 579 fields, representing repeated measurements in most cases. For instance, a field showing non-infested maize at the V9 growth phase might show moderately infested maize at the V12

Table 1. Field observations for the four selected maize growth phases.

Maize growth phase	Non infested	Moderately infested	Severely infested	Total
V9	43	121	81	245
V12	112	178	75	365
Silking	132	161	52	345
Maturing	195	100	25	320
Total	482	560	233	**1275**

growth phase, and so on. These observations were further categorized into two groups: 482 from non-infested and 793 from infested(Table 1).

2.3. FAW infestation grouping

FAW infestations are closely linked to significant crop damage, particularly in maize, where they can rapidly destroy large portions of the crop. This damage includes reductions in leaf area and general crop health. Several classification systems exist to evaluate the extent of infestation. In this study, the rank-and-class method (Toepfer et al. 2021) was used, based on two indicators: the number of small fresh windowpane injuries and the count of infested whorls. Maize samples were categorized into three classes following the same procedure as done by Dzurume et al. (2025).

2.4. Satellite data acquisition and pre-processing

Pre-processed Sentinel-1 and Sentinel-2 datasets were acquired from Google Earth Engine (GEE) for December 2019 to May 2020. GEE provides access to planetary-scale geospatial datasets and parallel cloud computing, which enables efficient processing of large volumes of remote sensing data without local computational resources. The methodology, including classification and feature extraction, was implemented using GEE's JavaScript. This facilitates rapid and repeatable analysis over extended spatial and temporal domains, making it suitable for integration into operational workflows (see Supplementary Figure S3).

The criteria for selecting satellite images was to obtain only satellite images available on the same day or immediately after the day that field observations were taken. For non-infested maize fields, images from the same day or up to 3 days before the field observations were also considered.

Sentinel 1 C-band SAR backscatter data were acquired in Interferometric Wide Swath mode (250 km wide) with dual-polarization (σ_{VH}^{o} and σ_{VV}^{o}) from GEE. Sentinel 1 provides σ_{VV}^{o} (vertical transmit-vertical receive) and σ_{VH}^{o} (vertical transmit-horizontal receive) polarizations. Sentinel 1 has a revisit period of 6–12 days and a spatial resolution of 10 metres. The imagery is pre-processed to Level-1 Ground Range Detected (GRD), which includes geometric corrections and orthorectification. Further processing in the GEE environment involved radiometric calibration to correct the backscatter values and speckle filtering with a focal median filter to reduce noise.

Sentinel-2 has a wide field of view (290 km), a high revisit frequency (5 days with two satellites), and high-resolution multispectral imagery (10 m, 20 m, and 60 m). It includes thirteen (13) spectral bands in the visible (492-665 nm), red-edge (704-783 nm), near-infrared (833-865 nm) and shortwave infrared (1614-2202 nm) domains. Pre-processing of Sentinel-2 data involved (1) removing bands 1, 9 and 10 and resampling the remaining bands to a resolution of 10 metres using bilinear interpolation and reprojected the data accordingly. (2) For Sentinel-2 imagery with less than 10% cloud cover, we used the QA60 band to apply a cloud-masking function, removing pixels affected by clouds and cirrus clouds. (3) We filtered the Sentinel 2 images by date and location. (4) The median pixel value for each Sentinel 2 band per growth phase was calculated. Studies have demonstrated that the median image compositing method yields comparatively better results than other methods, such as the maximum ratio value (Mudereri et al. 2022).

Sentinel-1 backscatter coefficients, together with Sentinel-2 reflectance bands and their derived spectral vegetation indices on the dates corresponding to the four maize growthphases, were selected to define the phenological phases. Despite occasional challenges from cloud cover exceeding 10%, the frequent 5-day revisit cycle of Sentinel-2, along with Sentinel-1's all-weather data acquisition capability, ensured the availability of sufficient cloud-free satellite imagery. Furthermore, the extended field observation period contributed to obtaining high-quality data for precise analysis.

2.5. Spectral vegetation indices (VIs)

Eight spectral vegetation indices (VIs), derived from Sentinel-2 images, were assessed based on their suitability for assessing crop health, chlorophyll, and water content (Table 2). These specific indices were chosen for their complementary ability to assess crop health, and stress levels with high sensitivity. Normalized Difference Vegetation Index (NDVI) serves as a baseline for vegetation vigour (Greene et al. 2021), while Modified Chlorophyll Absorption in Reflectance Index (MCARI) (Hoseny et al. 2023) and Red Edge Chlorophyll Index (RECL) enhance chlorophyll sensitivity, capturing stress-induced changes (-Gitelson et al. 2005).

Table 2. Spectral vegetation indices that were used in this study and their characteristics.

No.	Vegetation indices	Equation	Sentinel 2 bands used	Reference
1.	Normalized Difference Vegetation Index (NDVI)	(NIR-Red)/(NIR +Red)	(B8-B4)/(B8+B4)	Rouse et al., (1974)
2.	Modified Chlorophyll Absorption in Reflectance Index (MCARI)	((Red Edge 1 - Red) – 0.2 * (Red Edge 1 - Green))*(Red Edge 1/Red)	((B5 - B4) – 0.2 * (B5 – B3))* (B5/B4)	Daughtry et al., (1999)
3.	Red Edge Chlorophyll Index (RECL)	((NIR/Red Edge 1))-1	(B8/B5)-1	Gitelson et al. (2005)
4.	Modified Simple Ratio (MSR)	((NIR/Red) – 1)/sqrt((NIR/Red) + 1)	((B8/B4) – 1)/sqrt ((B8/B4) + 1)	Chen,1996
5.	Red Edge Position (REP)	705 + 35 * ((Red + Red Edge3)/2 – Red Edge 1/(Red Edge 2 – Red Edge 1))	705 + 35 * ((B4 + B7)/2 - B5/(B6 - B5))	Horler et al., 1983
6.	Red Edge Simple Ratio (RESR)	NIR/Red Edge	B8/B5	Gitelson and Merzlyak (1994)
7.	Red Edge Normalized Difference Vegetation Index (RENDVI)	(NIR – Red Edge 2)/(NIR + Red Edge 2)	(B8 – B6)/(B8+ B6)	Gitelson and Merzlyak (1994)
8.	Normalized Difference Red Edge Index (NDRE)	(NIR– Red edge 1)/(NIR+ Red Edge 1)	(B8 – B5)/(B8+ B5)	Barnes et al. (2000)

Modified Simple Ratio (MSR) improves canopy structure and biomass assessment, aiding in defoliation detection (Bhattarai et al. 2020). Red Edge Position (REP) detects early stress by tracking pigment shifts (-Fernández et al. 2020). The Red Edge Simple Ratio (RESR) was chosen for its ability to enhance sensitivity to chlorophyll content and canopy structure using the red-edge spectral region. It provides a refined assessment of vegetation stress and biomass, complementing other indices like NDVI and NDRE, while Red Edge Normalized Difference Vegetation Index (RENDVI) refines chlorophyll variation monitoring (Tao et al. 2022). Normalized Difference Red Edge Index (NDRE) assesses nitrogen and chlorophyll levels. Together, these indices provide a comprehensive approach to vegetation monitoring, combining general health assessment with early stress detection.

2.6. Derivatives from the satellite data

The mean σ_{VV}^{o}, σ_{VH}^{o} , and $\sigma_{VV}^{o}/\sigma_{VH}^{o}$ from Sentinel-1, along with reflectance values and VIs from Sentinel-2, were extracted for each infestation class at each growth phase. This was done to compare non-infested maize with maize exhibiting moderate and severe infestations using Kruskal–Wallis and Dunn's post-hoc tests. The Kruskal–Wallis test was chosen because it is a non-parametric test that does not require the assumption of normality and allows for comparison between multiple independent groups. Specifically, we generated and inspected histograms, boxplots, and Q – Q plots for each variable; none exhibited substantial skewness, kurtotic tails, or influential outliers. These visual assessments provided clear, intuitive confirmation of approximate normality and informed the decision to proceed with subsequent parametric analysis. Since the data does not follow a normal distribution, this test provides a more appropriate alternative to ANOVA. We used the Kruskal–Wallis (Kruskal and Wallis 1952) to assess statistical differences ($p < 0.05$) of the sample means among the FAW infestation classes. When significant differences were found, Dunn's post-hoc test was applied to conduct pairwise comparisons among classes (Dunn 1964).

2.7. RF and SVM classification

Two classifiers were used: a Support Vector Machine (SVM) and a Random Forest (RF) classifier to classify the three classes of FAW infestation with individual models for each phase. RF uses decision trees, which classify data points by navigating through a structured series of decisions until the criteria for assigning a class are fulfilled (Breiman 2001). SVM uses support vectors, which are the critical data points closest to the decision boundary, to define an optimal hyperplane that separates classes by maximizing the margin between them (Cortes et al.1995).

The hyperparameters for the SVM and RF classifiers were selected based on a combination of standard practice and performance accuracies. For the SVM, an RBF kernel was used with gamma = 10 and C = 100 after parameter tuning (https://developers.google.com/earth-engine/apidocs/ee-classifier-libsvm.) to capture complex, non-linear decision boundaries often present in remote sensing data (Adugna et al. 2022). These values reflect a balance between model complexity and classification accuracy, based on prior experience and reported effectiveness in similar classification (Goyal et al. 2024). The RF model has two key tuning parameters: the number of trees in the ensemble, referred to as ntree, and the number of predictors used to split nodes, referred to as mtry (https://developers.google.com/earth-engine/apidocs/ee-classifier-smilerandomforest). For the RF classifier, 100 trees were used to ensure model stability without incurring excessive computational cost. The variablesPerSplit (mtry) parameter was dynamically set to the minimum of the total number of input bands, a conservative strategy to reduce overfitting when working with high-dimensional multispectral and SAR data (Banks et al. 2019). The chosen parameters are consistent with well-established practices in remote sensing classification workflows (Belgiu and Drăgu 2016)

To address class imbalance, a class-weighting strategy was employed during model training (He and Garcia 2009). Class frequencies were computed from the training data, and each class was assigned a weight inversely proportional to its frequency using the class_weight='balanced' setting in GEE. This approach ensures that minority classes are given more importance by the classifier during training without modifying the data distribution through resampling (Carvalhoet al. 2025) A five-fold cross-validation strategy ($k = 5$) was implemented to assess classifier robustness. The data were randomly partitioned by generating a random column, with each fold defined by sequentially selecting a test subset and using the remainder for training. Both classifiers were applied for each fold, and performance metrics (cross-validation accuracy, test accuracy, and F1 score) were computed using confusion metrics. These metrics were averaged across the folds to yield robust performance estimates. The SVM and RF classifiers were trained on a 70% stratified subset of the data and evaluated on a 30% independent validation set. The class-weighting approach contributed to more balanced performance across classes, as reflected in improved F1 scores for minority classes.

2.8. *Feature importance*

The feature importance of each variable was calculated using the permutation importance measure (Zhang and Yang 2020). This method evaluates how each predictor variable contributes to accuracy improvements in the optimized classification model, expressed as a normalized percentage contribution. Finally, the performance of both classifiers was assessed by comparing the predicted classifications with ground truth data and reporting the overall accuracy (OA) and F1-score. Compared the performance of RF and SVM across four maize growth phases using five different input datasets: (i) Sentinel 1 only, (ii) Sentinel 2 bands only, (iii) Sentinel 2 bands and VIs, (iv) Sentinel 2 bands combined with Sentinel 1, and (v) a combination of Sentinel 1, Sentinel 2 bands, and VIs.

3. Results

3.1. *Assessing FAW class separability through Sentinel 1 polarizations*

Figure 5 presents backscatter values (in decibels, dB) across four crop growth phases (V9, V12, silking, maturing) under three infestation classes (non-infestation, moderate infestation, severe infestation) for $\sigma_{VH}°$, $\sigma_{VV}°$, and $\sigma_{VH}°/\sigma_{VV}°$. In $\sigma_{VH}°$, severe infestations tend to have slightly higher backscatter values, particularly in the silking (around −14 dB) and maturing phases (around −13 dB), while non-infested crops show larger variability in V9 (ranging from approximately −18 dB to −12 dB). In $\sigma_{VV}°$, severe infestations exhibit higher

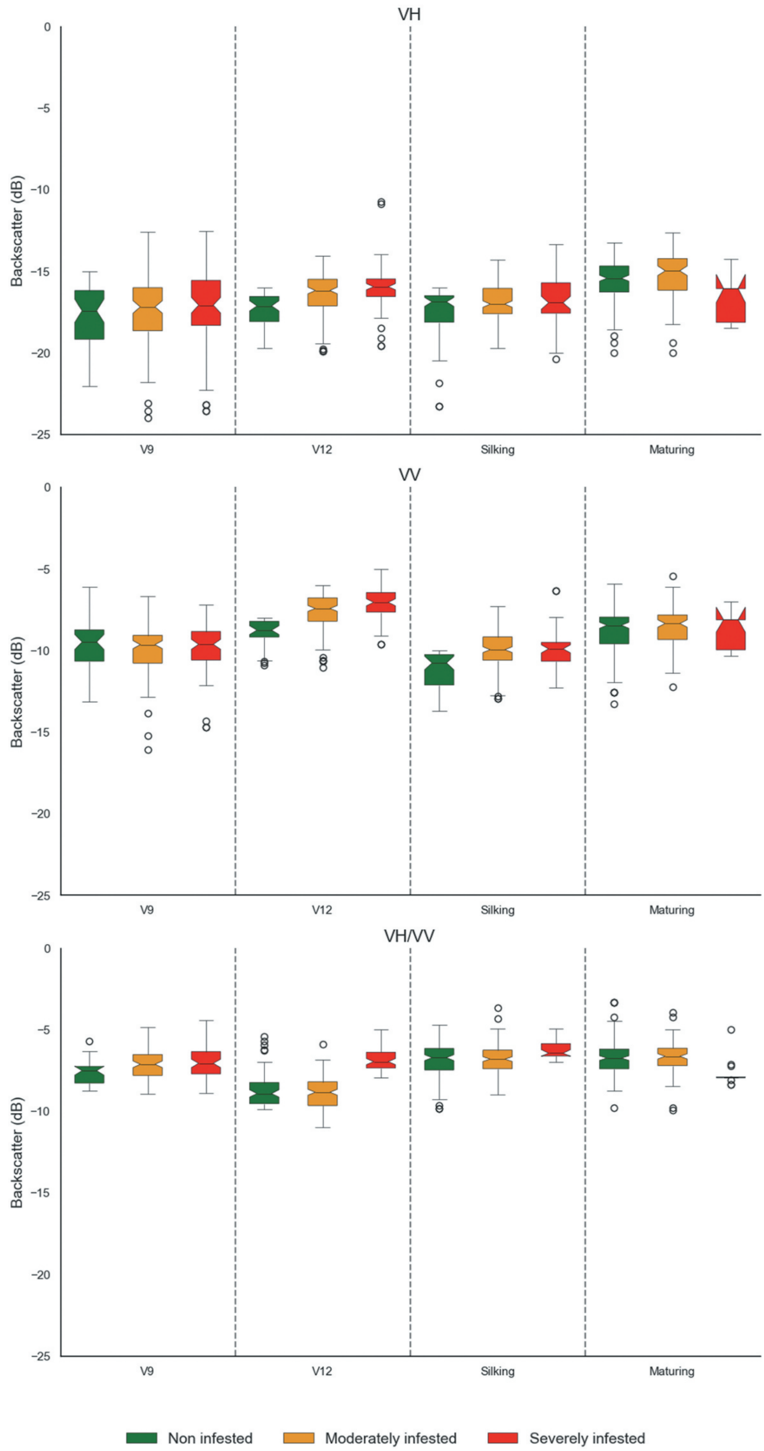

Figure 5. Box plots representing variations in σ_{VH}^o, σ_{VV}^o and $\sigma_{VH}^o/\sigma_{VV}^o$ for the four different maize growth phases for the three classes of FAW infestation.

Table 3. Kruskal–Wallis with Dunn's post-hoc test for significant differences in σ_{VH}^{o}, σ_{VV}^{o} and $\sigma_{VH}^{o}/\sigma_{VV}^{o}$ across the infestation classes.

Phase	Infestation Class 1	Infestation Class 2	σ_{VH}^{o}	σ_{VV}^{o}	$\sigma_{VH}^{o}/\sigma_{VV}^{o}$
			p-value		
V9	NI*	MI	**0.041**	0.309	**0.029**
	MI	SI	0.374	0.619	0.457
	NI	SI	0.187	0.640	**0.012**
V12	NI	MI	**<0.01**	**<0.01**	0.585
	MI	SI	0.160	**<0.01**	**<0.01**
	NI	SI	**<0.01**	**0.010**	**<0.01**
Silking	NI	MI	0.066	**<0.01**	0.735
	MI	SI	0.098	**<0.01**	**<0.01**
	NI	SI	0.034	0.660	**<0.01**
Maturing	NI	MI	**0.010**	0.107	0.288
	MI	SI	**0.010**	0.535	**<0.01**
	NI	SI	0.060	0.160	**<0.01**

$p < 0.05$ in **bold**. *NI = Non infested, MI = Moderately infested, SI = Severely infested.

backscatter at V9 (around −10 dB) and V12 (around −9 dB), but differences among infestation levels narrow in the silking and maturing phases, converging around −10 dB. For the $\sigma_{VH}^{o}/\sigma_{VV}^{o}$, severe infestations maintain slightly higher backscatter, especially in V9 (about −6 dB) and V12 (about −5 dB), with minimal differences across infestation levels by the silking and maturing phases (around −7 dB). As shown in Table 3, the Kruskal–Wallis test revealed significant differences in σ_{VV}^{o} backscatter across infestation classes, with σ_{VH}^{o} also demonstrating strong significance. Notably, the $\sigma_{VH}^{o}/\sigma_{VV}^{o}$ ratio was particularly sensitive, displaying significant differences at V9 ($p = 0.029$), V12 ($p < 0.01$), and Silking ($p < 0.01$).

3.2. Variations in Sentinel 2 spectral reflectance

Figure 6 shows the mean spectral reflectance for six bands (red (665 nm), red edge (704-783nm) - and near-infrared (833-865)) by FAW infestation class and growth phase. Across red (665 nm) and red-edge 1 (704 nm), reflectance values were consistently higher under severe infestation, with the greatest differences observed during the V12, silking and maturing phases. The near-infrared band showed increased reflectance with no infestation, particularly during the V12 and silking phases. Moderate and no infestation levels were generally closer but distinguishable. As shown in Table 4, the Kruskal–Wallis test identified red edge 3, - and near-infrared as the most sensitive bands for distinguishing infestation classes. Red edge 3 (783 nm) and narrow near-infrared (865 nm) consistently excelled across comparisons, with high sensitivity for non-infested versus moderately infested and moderately infested versus severe infestation. Red edge 1 (704 nm) and 2 (740 nm) showed moderate sensitivity in some cases. Red-edge 3 (783 nm) and near-infrared (833 nm) were consistently the most distinguishing bands across classes.

3.3. Spectral vegetation indices

Figure 7 and Table 5 represents the mean values of the eight VIs corresponding to the three classes of FAW infestation. The vegetation indices showed distinct patterns

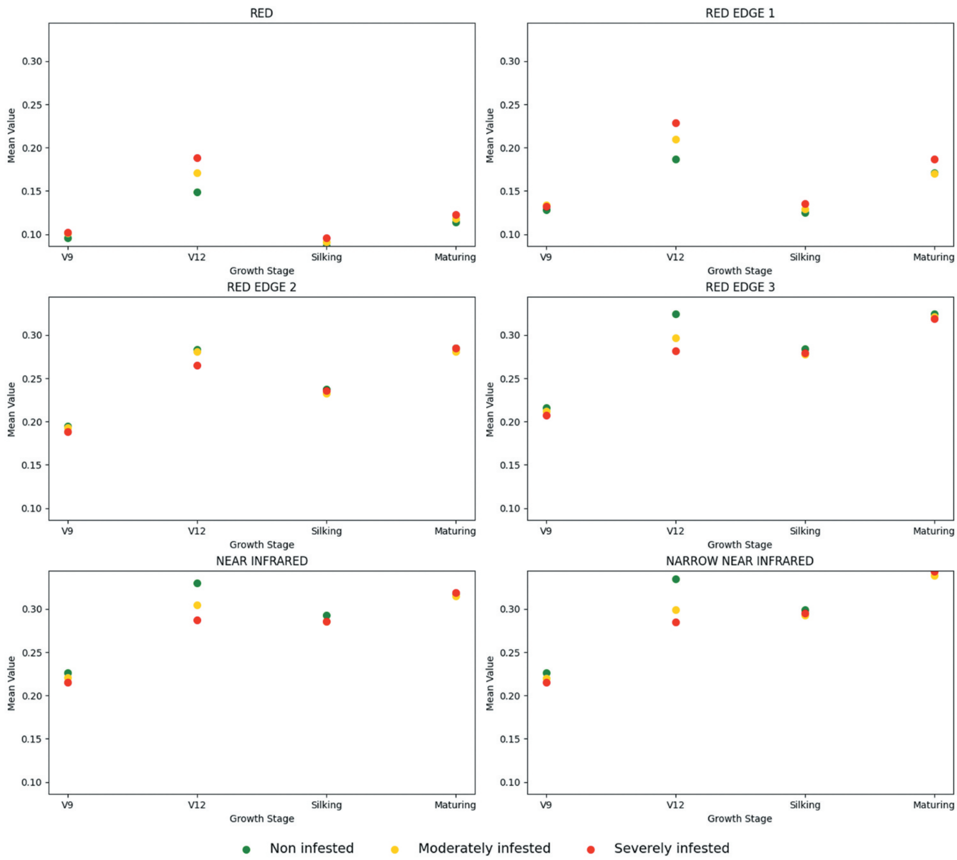

Figure 6. Mean reflectance patterns across spectral bands (red, red edge -, and near-infrared) by growth phases and FAW infestation class.

across infestation classes and growth phases. NDVI, MCARI, NDRE, and MSR emerged as the most effective for distinguishing between FAW infestation classes. RECL and RENDVI showed minimal variation among classes, though non-infested maintained slightly higher values. Significant differences ($p < 0.05$) in VI across growth phases and infestation classes were identified using the Kruskal–Wallis test. MCARI was notably significant at the V12 phase ($p < 0.001$) and during silking. RESR and NDRE showed significant differences across multiple phases, including V9, V12, and silking ($p < 0.001$) as shown in Table 5.

3.4. *Variable importance*

Figure 8 presents the relative importance of each spectral feature and index at four maize growth phases (V9, V12, Silking, and Mature). Across all growing phases, the σVHo SAR band (Filtered_VH) consistently exhibits the highest importance. Several red-edge and shortwave infrared (SWIR) bands (e.g. RE2, RE3, SWIR1, and SWIR2) and common vegetation indices (NDVI, NDRE, and RENDVI) also show up repeatedly among the top variables, but their relative ranking changes across phases. At early phases (V9, V12), certain narrow-band indices (e.g. RE2, RE3, and MCARI) become especially important, whereas at later

Table 4. Kruskal–Wallis with Dunn's post-hoc test for significant differences across spectral bands.

Phase	Infestation Class 1	Infestation Class 2	Red	Red Edge 1 (RE1)	Red Edge 2 (RE2)	Red Edge 3 (RE3)	Near-infrared (NIR)	narrow Near-infrared (nNIR)
V9	NI*	MI	0.166	0.134	0.556	**<0.01**	0.333	**0.014**
	MI	SI	0.035	0.057	**<0.01**	0.377	0.611	0.437
	NI	NI	0.073	0.444	**<0.01**	0.176	0.633	**<0.01**
V12	NI	MI	0.051	0.070	**<0.01**	**<0.01**	**<0.01**	0.614
	MI	SI	**<0.01**	**<0.01**	**<0.01**	0.198	**<0.01**	**<0.01**
	SI	SI	**<0.01**	**<0.01**	0.070	**<0.01**	**<0.01**	**<0.01**
SIking	NI	MI	**<0.01**	**<0.01**	**<0.01**	0.022	**<0.01**	0.770
	MI	SI	**<0.01**	**0.012**	**<0.01**	0.712	0.651	**<0.01**
	NI	SI	**<0.01**	0.470	0.518	0.147	**<0.01**	**<0.01**
Maturing	NI	MI	0.463	**<0.01**	0.804	**<0.01**	0.040	0.252
	MI	SI	**<0.01**	**<0.01**	0.849	**<0.01**	0.310	**<0.01**
	NI	NI	**<0.01**	**0.024**	0.9859	**0.042**	0.896	**<0.01**

$p < 0.05$ in **bold**. *NI = Non infested, MI = Moderately infested, SI = Severely infested.

Table 5. Kruskal–Wallis with Dunn's post-hoc test for significant differences across VIs.

Growth phase	Infestation Class 1	Infestation Class 2	NDVI	MCARI	MSR	NDRE	RECL	RENDVI	RESR	REP
V9	NI*	MI	0.138	0.028	0.022	0.010	0.556	0.675	0.088	0.973
	NI	SI	0.057	**<0.01**	0.022	0.011	**<0.01**	0.012	0.087	0.885
	MI	MI	0.444	0.012	**<0.01**	**<0.01**	**<0.01**	**<0.01**	0.226	0.227
V12	NI	MI	0.064	**<0.01**	**<0.01**	**<0.01**	**<0.01**	**<0.01**	0.017	0.079
	NI	NI	**<0.01**	0.097	**<0.01**	**<0.01**	**<0.01**	**<0.01**	0.01	0.634
	MI	SI	**<0.01**	0.100	**<0.01**	0.164	0.066	**<0.01**	0.640	0.881
Silking	NI	MI	**<0.01**	0.011	**<0.01**	0.949	**<0.01**	**<0.01**	**<0.01**	0.600
	NI	SI	0.012	0.137	**<0.01**	**<0.01**	**<0.01**	**<0.01**	0.095	0.091
	MI	SI	0.470	**<0.01**	0.241	**<0.01**	0.515	0.531	0.940	0.225
Maturing	NI	NI	**<0.01**	0.458	**<0.01**	0.034	0.800	**<0.01**	0.167	0.720
	NI	SI	**<0.01**	**<0.01**	**<0.01**	**<0.01**	0.849	**<0.01**	0.453	0.705
	MI	MI	0.024	0.022	0.241	**<0.01**	0.985	**<0.01**	0.290	0.455

$p < 0.05$ in **bold.** *NI = Non infested, MI = Moderately infested, SI = Severely infested.

growing phases (Silking and Mature) certain features gain prominence alongside SAR-based VH.

3.5. Classification

Accuracy assessment of FAW infestation classes across four growth phases is performed by comparing satellite-derived backscatter and spectral reflectance with field observations (Table 6). Classification accuracy varied across growth phases, data sets, and models, as shown in Table 6. Using only the Sentinel 1 features during the V9 phase, the RF classifier achieved a cross-validation accuracy of 94%, a test accuracy of 96%, and an F1 score of 92%, while the SVM recorded notably lower values of 78%, 80%, and 71%, respectively. However, when multiple data sources were integrated, particularly with the Sentinel1+Sentinel2+VIs combination, both classifiers exhibited marked performance improvements. Under this configuration, RF reached up to 96% cross-validation and test accuracies with F1-scores ranging between 92% and 97% across phases, and SVM similarly attained accuracies in the mid-90s, with an F1-score peaking at 98% in the V12 phase. The best performing model at each growth phase was used to generate infestation maps per growth phase (see Supplementary Figure S1 and S2).

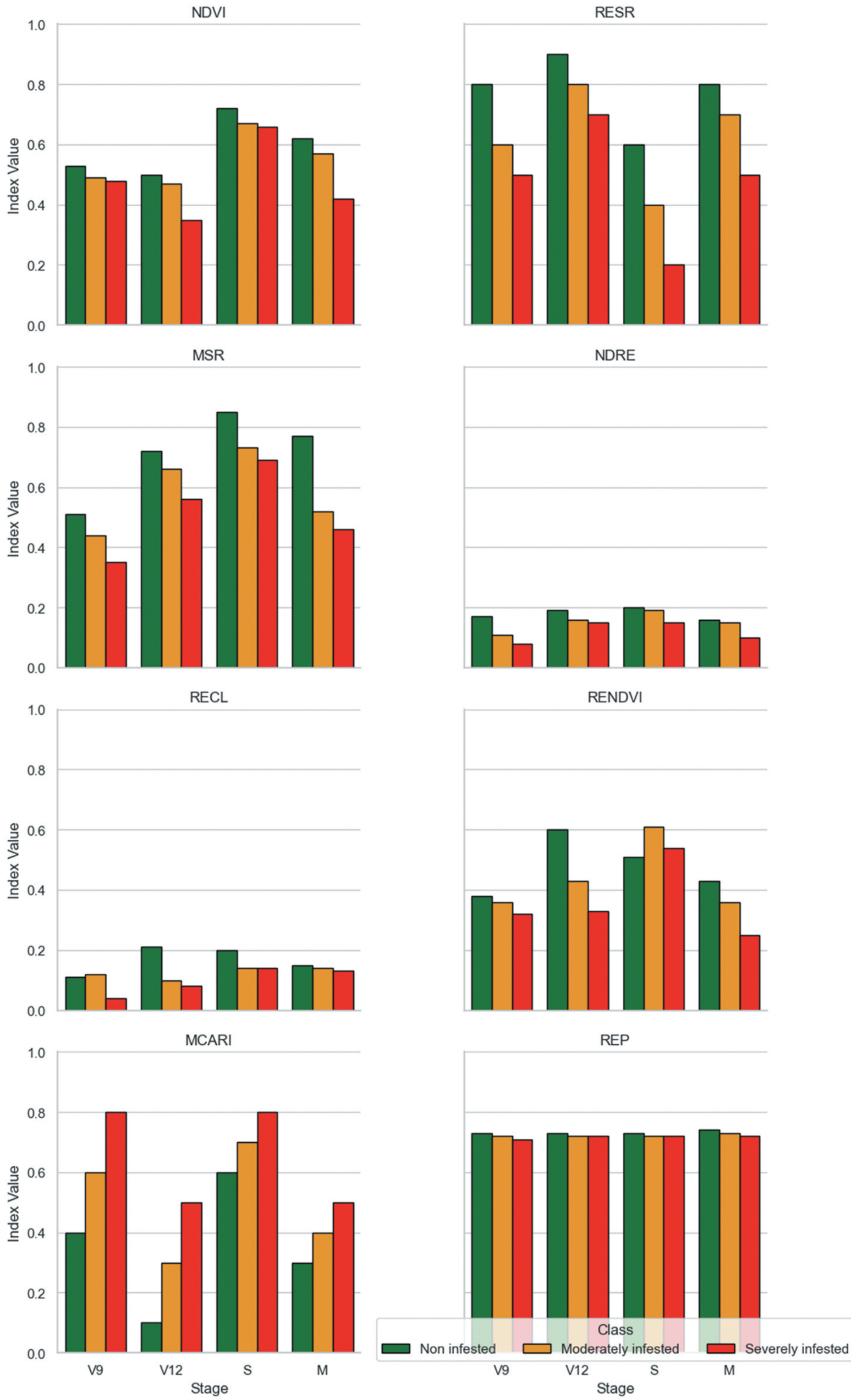

Figure 7. Average vegetation index values across four maize growth phases for three classes of infestation.

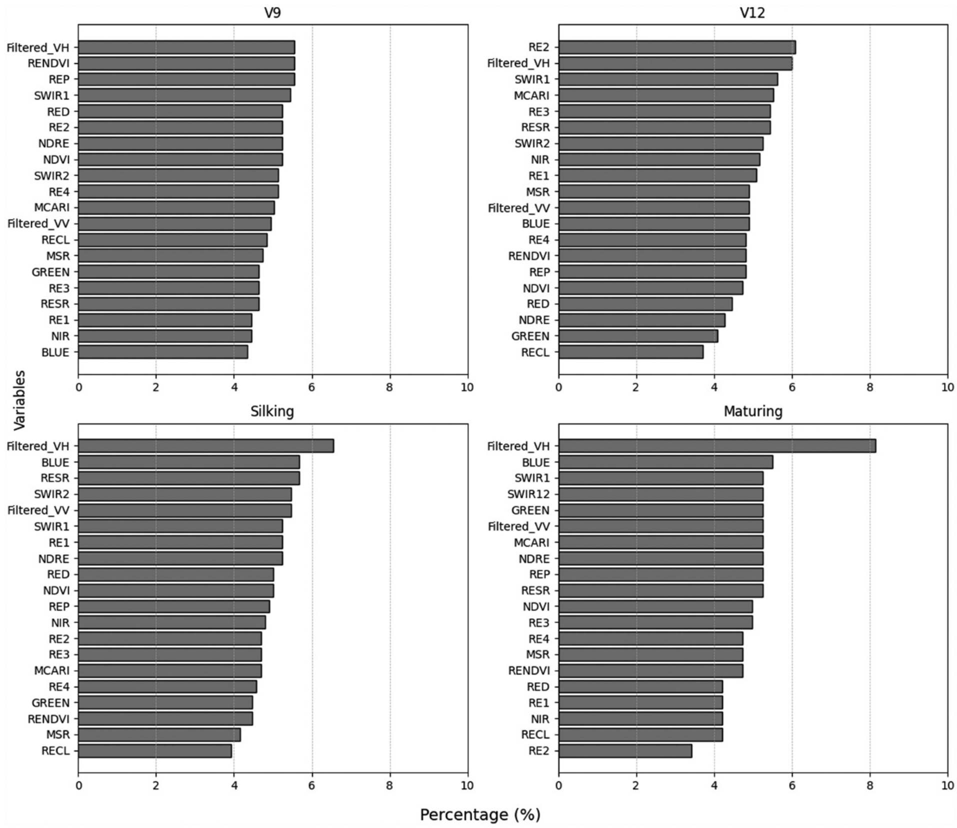

Figure 8. Feature importance of spectral and SAR features for maize FAW infestation at four phenological phases.

4. Discussion

The integration of optical and SAR EO data with ML classification models and sufficient field reference data for model training is a robust means of estimating FAW infestation intensity in maize over large geographic areas. In this study, freely available satellite data were used to characterize FAW infestation in maize. FAW infestation classification performance was evaluated across five combinations of freely available EO data, two ML algorithms, and four growth phases. These methods were validated through field observations of FAW infestations, providing useful insight into suitable EO-based variables and methods for detecting and classifying FAW infestation intensity.

4.1. Infestation impacts on backscatter across the maize growth phase

SAR-based parameters capture structural changes in the maize crop that can be associated with FAW infestation. In general, for the V9 and V12 phases, the differences in backscatter between FAW infestation classes were minimal, particularly for the σ_{VH}^{o} and $\sigma_{VH}^{o}/\sigma_{VV}^{o}$. This trend can be attributed to the fact that the crop is still developing during these phases, and the structural changes caused by the infestations may not

Table 6. RF and SVM classifiers' performance across maize growing phases (V9, V12, silking and mature) and evaluation metrics.

		Metrics and phases											
		Cross validation accuracy	Test accuracy	F1-score	Cross Validation accuracy	Test accuracy	F1-Score	Cross validation accuracy	Test accuracy	F1-Score	Cross validation accuracy	Test accuracy	F1-score
Classifier	Combination	V9			V12			Silking			Mature		
RF	Sentinel 1	94	96	92	94	92	93	92	90	92	90	88	89
SVM	Sentinel 1	78	80	71	70	70	66	65	61	61	81	79	83
RF	Sentinel 2	90	86	87	88	88	86	88	86	86	84	77	81
SVM	Sentinel 2	90	92	92	87	93	90	88	90	90	83	80	86
RF	Sentinel 1+Sentinel 2	95	95	91	94	93	93	93	92	90	85	84	83
SVM	Sentinel 1+Sentinel 2	95	96	96	95	91	97	93	93	94	85	84	89
RF	Sentinel 2+VIs	91	90	86	88	86	86	88	86	86	84	87	81
SVM	Sentinel 2+VIs	90	93	92	88	83	90	88	89	90	84	80	86
RF	Sentinel 1+Sentinel 2 +VIs	96	96	92	95	96	92	92	96	97	84	88	97
SVM	Sentinel 1+Sentinel 2 +VIs	96	96	97	95	93	98	93	96	94	84	91	88

yet be sufficiently pronounced to affect C-band backscatter signals significantly. At the silking phase, $\sigma_{VH}°$, backscatter values for severely infested crops were slightly higher than those for non-infested and moderately infested crops. This suggests that structural changes in the canopy (e.g. reduced biomass or altered crop orientation due to severe infestation) can influence the SAR signal. Similarly, $\sigma_{VV}°$ also exhibited distinctive differences between the three infestation classes at this phase, with severe infestations showing higher backscatter values than non-infested and moderately infested crops. During the maturing phase, noticeable differences in backscatter across the infestation levels, particularly under $\sigma_{VV}°$, exhibited explicit differentiation among infestation classes. This could be attributed to the fact that the temporal behaviour of SAR signals reflects not only the changes between growth phases but also variations in water content and environmental conditions (Kaushik et al. 2021). The $\sigma_{VH}°/\sigma_{VV}°$ also showed significant differences at this phase, indicating that combining both polarizations might enhance the detection of infestation levels during later growth phases. Due to its ability to acquire data in all weather conditions, Sentinel 1 data can be used to monitor FAW infestation classes during the entire phenological cycle. Differences between backscatter and infestation levels became more distinct at later phases of development (Figure 5), underscoring the potential of SAR data as a valuable tool for monitoring crop health and detecting FAW infestation.

4.2. Sentinel-2 spectral bands trends

Pest damage can induce structural and physiological changes in crops, directly and indirectly influencing canopy spectral reflectance specifically in the visible and near-infrared regions (Ribeiro et al. 2024). In this study, six Sentinel2 spectral bands were selected ranging from red to narrow near infrared to evaluate their ability to differentiate between three classes of FAW infestation. Previous studies, such as those by Kumbula et al. (2019), Jia et al. (2023) and Dzurume et al. (2025) have shown that red-edge bands slightly outperform other spectral bands in detecting insect pests in agricultural and forestry applications, aligning with the findings of this study. The red and near-infrared bands showed a stronger sensitivity to FAW infestation damage, agreeing with Zhang et al. (2016). The differences in the spectral data are especially noticeable in the near-infrared and the red-edge regions. The near-infrared band consistently shows the largest differences in reflectance between different phases and infestation levels. This may suggest the use of bands in infrared and red edge to detect stress or health status in crops since non-infested crops tend to reflect more in this region due to their chlorophyll content and developed canopy structure. In addition, Ribeiro et al. (2024) demonstrated a significant effect of the soybean aphid on three bands, e.g. red-edge 2, 3 and narow near infrared. Similarly, in this study, the red-edge bands proved crucial in classifying the three FAW infestation classes, showing these bands' importance.

The analysis showed that, the red-edge and shortwave-infrared bands consistently ranked among the most important bands, while among indices, NDVI and MCARI exhibited the highest separability between classes. This could be attributed to the sensitivity of the red-edge to crop stress and early physiological disruptions (Abdullah et al. 2019; Eitel et al. 2011). Further variations in water content, leaf dry matter and leaf area index (LAI) alter reflectance in the SWIR region (Ali et al. 2017; Darvishzadeh et al. 2009). For example, the study that was done by Abdullah et al. (2019) showed that the red-edge and SWIR were important spectral regions at both leaf and canopy levels for detecting subtle changes in Norway spruce trees due to bark beetle infestation. These findings align with previous studies that have demonstrated (i) red-edge's ability to detect stress and (ii) the superior performance of NDVI and MCARI over single-band or less targeted indices in crop health monitoring (Haboudane et al. 2002; Zarco-Tejada et al. 2004).

The red-edge region refers to the narrow spectral region where there is a sharp increase in crop reflectance due to the transition between chlorophyll absorption in the red wavelengths and high reflectance in the near-infrared. This region has been shown in many studies to be sensitive to crop stress conditions and is particularly sensitive to changes in chlorophyll content and canopy structure, making it a valuable indicator for assessing crop health and stress. Crop stress often leads to shifting the position of the red edge towards shorter wavelengths (blue shift), mainly due to changes in chlorophyll and other pigments concentration before visible symptoms appear. Red-edge indices are frequently used in remote sensing for early crop stress detection and monitoring crop dynamics (Mutanga and Skidmore 2004).

4.3. Spectral vegetation indices (VIs) to detect FAW infestation

VIs are important in identifying the physiological changes in maize canopy structure, such as chlorophyll content and reduction in the leaf area. Eight VIs were used to discriminate non-infested and infested maize. The VIs included either red-edge bands alone or a combination of red-edge and near-infrared bands. The chosen VIs are sensitive to changes in crops' biophysical and biochemical characteristics. Overall, most VIs decreased with increasing infestation levels, which is attributed to the strong relation between these VIs and chlorophyll content (Lu et al. 2022). 2023 By contrast, MCARI showed the opposite pattern, MCARI increases as chlorophyll concentration decreases, so higher MCARI values indicate lower chlorophyll levels (Daughtry et al.1999).

The results highlight the importance of the red-edge domain for mapping pest defoliation, aligning with earlier observations reported by studies conducted by Oumar and Mutanga, 2014 and Bhattarai et al. (2021). The results also concur with the findings of Adan et al. (2023), who used spectral VIs, such as NDVI, to monitor crop health and vigour in the presence of FAW infestations. Their study demonstrated a decline in NDVI values from 2017 to 2020 due to the impact of FAW infestations. The findings are consistent with numerous studies that have successfully applied Sentinel 2 based vegetation indices to monitor pest-induced changes across various ecosystems. For example, Abdullah et al. (2019); in temperate forest, Prabhakar et al. (2022) in sorghum farm fields and Ramos et al. (2022) in cotton fields. More specifically, a study that was done by Kara et al. (2023) using Sentinel 2 and VIs, to analyse the damage caused by beet webworm moths (*Loxostege sticticalis*) in sunflower fields concluded that Enhanced Vegetation Index was the most effective indicator of damage among the crop indices.

4.4. FAW infestation classification

This study evaluated the relative performance of two commonly used ML classifiers, RF and SVM, for classifying FAW infestation. RF is more robust with larger datasets due to its ensemble learning approach, which can handle more complex and non-linear relationships between the input variables. The accuracy assessment evaluates the reliability of FAW infestation classifications across four distinct growth phases. This process involves comparing satellite-derived data with ground-based field observations at each phase. By analysing backscatter, spectral reflectance patterns, VIs captured in satellite imagery and correlating them with field measurements, the assessment ensures consistency and accuracy in infestation classification. The Sentinel1, Sentinel2, and VIs combination improved accuracy for all maize growth phases. All variables (Sentinel1, Sentinel2, and VIs) demonstrated high effectiveness in capturing distinct changes across all four maize growth phases. Their combined use enhances the detection of biochemical, structural, and spectral variations, which are critical for assessing crop health and yield loss. In fact, combining these datasets offers the most robust assessment by comprehensively capturing the changes that impact yield.

Integrating Sentinel1, Sentinel2, and VIs improves detection by addressing biochemical alterations (such as chlorophyll loss) as well as structural damage, while VIs provide valuable insights into overall crop health. This is similar to a study by Bhattarai et al. (2021), where they mapped Spruce budworm host species using Sentinel1 SAR, Sentinel2 imagery, and an RF classifier. The best model, using Sentinel 2 bands and VIs, achieved 72.6% accuracy and a kappa of 0.65. Adding Sentinel 1 and elevation slightly improved performance (73.0% accuracy, 0.66 kappa), while using only Sentinel 1 and elevation gave lower accuracy (57.5%).

ML classifiers can yield inconsistent results due to various factors, including challenges in hyperparameter tuning, data source selection, training sample quality, imbalanced class distributions, and feature selection, all of which influence their reliability and performance (Mudereri et al. 2022). To enhance the performance and reliability of our model, we conducted hyperparameter tuning, optimizing key parameters to ensure the best possible results. This process was crucial in improving classification accuracy and mitigating inconsistencies in model performance. RF performed better than SVM across most metrics, particularly in cross-validation accuracy and test accuracy. For example, using Sentinel 1 alone, RF achieves a 94% accuracy compared to SVM's 78%. While both models improve with additional features, such as in the Sentinel 1+Sentinel 2+VIs combination where both reach around 96% accuracy, SVM's F1-score increases notably, indicating its sensitivity to feature selection. Overall, RF demonstrates stable performance across various phases, making it the more robust classifier.

The key variables identified were several red-edge and SWIR bands (e.g. RE2, RE3, SWIR1, and SWIR2) and common vegetation indices (NDVI, NDRE, and RENDVI), which consistently showed significant contributions across all growth phases. In addition to showcasing the most important variables at each growth phase, Figure 8 reveals how the relative importance of various spectral regions and SAR polarizations shifts over time. For instance, while Filtered_VH (σ_{VH}^{o}) consistently remains dominant, red-edge indices (such as RENDVI, REP, and NDRE) and SWIR bands frequently appear among the top features throughout the cycle. This indicates that both chlorophyll-related (red-edge) and water-content/structural (SWIR) information are essential across all phases. In this study, the feature importance of RF and SVM resulted in a reasonable number of features for the classifications; hence, other feature selection methods, such as recursive feature elimination, were not considered, due to their high computational costs (Guyon et al. 2002).

FAW infestation differs by growth phase, ranging from subtle biochemical changes in early phases to pronounced structural in later phases (Day et al. 2017; Zhang et al. 2016). Notably, the slight changes in the ranking of red-edge and SWIR features from V9 to Mature suggest that their sensitivity to biomass, chlorophyll content, and water status evolves with phenological progression, whereas the persistently high ranking of SAR σ_{VH}^{o} underscores the value of SAR-derived structural information.

Misclassification in pest-related studies can be attributed to several factors. Variations in environmental conditions, such as differences in lighting, background clutter, and crop growth phases, can lead to misclassification. Additionally, pests often cause symptoms that overlap with those of other stresses or even healthy crops, making it challenging to extract distinguishing features. Maize crops at V9, V12, silking, and maturing phases have markedly different leaf and canopy structures. These natural variations can change how infestation symptoms appear, sometimes making moderate infestations appear similar to non-infested or severely infested. The visual difference between moderate and severe infestation may be subtle, especially if the symptoms develop gradually or vary due to environmental factors. This can cause overlap in the feature space, leading to misclassification. As Mohanty et al. (2016) reported, variations in crop morphology due to differences in growth phases can lead to classification errors. Integrating satellite data with ancillary environmental information, such as soil characteristics, is recommended to further improve classification robustness and accuracy.

4.5. Comparison of Sentinel 1 and Sentinel 2 data for detecting and mapping FAW infestation

Integrating Sentinel1 and Sentinel2 data significantly enhances pest detection by harnessing the complementary strengths of SAR and optical sensors. Sentinel1's SAR delivers reliable, all-weather imagery that captures crucial surface roughness and moisture variations, which are key indicators of vegetation stress due to pest activity. On the other hand, Sentinel2's high-resolution multispectral imagery detects subtle spectral changes associated with crop health. This synergistic approach enables continuous monitoring and early detection of pest infestations, allowing for targeted interventions that minimize crop damage and optimize resource use.

Recent advances in both optical and SAR-based remote sensing have further demonstrated the utility of Sentinel 1 and 2 for timely pest detection across diverse cropping systems. Della Bellver et al. (2024) applied Sentinel 2 MSI to detect mealybug (*Delottococcus aberiae*) infestations in citrus orchards, achieving robust classification with red edge and NDVI-derived indices. In soybean, Ribeiro et al. (2024) developed an economic threshold based LSVM model using Sentinel 2 bands to classify soybean aphid (*Aphis glycines*) outbreaks, reporting 91% accuracy, 85.7% sensitivity, and 93.3% specificity. On the SAR side, Sári-Barnácz et al. (2023) combined Sentinel 1 C-band backscatter with Sentinel 2 time series to map cotton bollworm (*Helicoverpa armigera*) damage in maize, demonstrating that fusion of optical and SAR features improves early detection in cloudy climates. Earlier foundational work by Mandal et al. (2020) introduced a Compact Polarimetric Radar Vegetation Index (CpRVI) from Sentinel 1 data and demonstrated its strong correlation with LAI and biomass across multiple crops, establishing SAR as a viable proxy for biophysical parameter retrieval. Veloso et al. (2017) compared the Sentinel 1 backscatter ratio (σ_{VH}o/σ_{VV}o) against Sentinel 2 NDVI across key European crops, revealing that SAR and optical indices capture complementary phenological signals, particularly during senescence and postharvest residue phases, thus underscoring the value of multisensor fusion for comprehensive crop monitoring. These recent studies, alongside the earlier SAR-specific applications, underscore that jointly exploiting Sentinel1's cloud penetrating C band backscatter and Sentinel 2's bands capabilities can significantly enhance operational pest surveillance.

In this study, the three FAW infestation classes could be detected and classified using the optical and SAR data, which shows that the two datasets offer complementary information on FAW infestation. The interpretation and the statistical differences of Sentinel1 polarizations and Sentinel2 spectral bands and indices in the above sections clearly show the best features that are critical for understanding the three classes of FAW infestation. As shown in Figure 5 and 6 the red edge, σ_{VV}^{o} and σ_{VH}^{o} are able to distinguish the three classes of FAW infestation across the four maize growth phases. The σ_{VH}^{o} is particularly sensitive to volume scattering from the vegetation canopy (e.g. its structure, moisture, and biomass). As a crop matures, its canopy generally becomes more complex. If pest infestation alters this structure (for instance, through defoliation, reduced biomass, or moisture changes), the σ_{VH}^{o} may respond more noticeably (Mandal et al. 2020). This can make the σ_{VH}^{o} increasingly important for detecting stress or damage in later growth phases. These results emphasize the value of integrating multi-source remote sensing data for effective and precise pest monitoring.

Other studies such as done by Feng et al. (2022) fused hyperspectral, thermal infrared and RGB data from a Unmanned Aerial Vehicles (UAV) to monitor wheat powdery mildew, showing that adding canopy-temperature information significantly improved detection of non-visual symptoms. However, flights were constrained to clear weather and low wind speeds, and processing thermal imagery demands rigorous radiometric calibration. Francesconi et al. (2021) combined thermal and RGB UAV imagery with gene-expression analyses to detect and physiologically characterize Fusarium head blight in durum wheat, achieving early detection but requiring costly molecular validation and close-range flights. These highlighted challenges underscore the importance of freely available EO data.

While this study centres on maize and FAW, Sentinel 1/Sentinel 2 fusion approaches have demonstrated strong potential across other crop/pest systems. For instance, Fu et al. (2022) successfully monitored cotton aphid severity using Sentinel 2 MSI data processed with a derivative of ratio spectroscopy algorithm and an RF model, achieving an overall classification accuracy of 80%. Similarly, Ruan et al. (2021) employed time series Sentinel 2 imagery combined with vegetation indices and an SVM to predict wheat stripe rust occurrence, reporting up to 86.2% prediction accuracies. These studies illustrate that by recalibrating spectral radar thresholds and retraining classifiers on minimal labelled samples, our framework could be adapted to detect damage in rice (e.g. stem borers) or other cereals with comparable efficacy. Such a transfer learning strategy leverages freely available Sentinel archives to scale across diverse geographies and pests, thereby significantly enhancing the general applicability of our remote sensing workflow.

One of the primary challenges associated with optical data is the lack of spatial and temporal continuity caused by cloud cover. However, the ability of SAR to traverse clouds demonstrates how these datasets can complement one another, enhancing the overall analysis and improving data continuity. Readily available Sentinel satellite imagery is an important tool for early pest detection and management, helping policymakers identify high-risk areas, implement timely actions, and promote sustainable pest management strategies to protect maize production and reduce economic losses

5. Limitations

While the results demonstrate the utility of Sentinel 1, Sentinel2 bands and VIs for FAW classification, several limitations must be acknowledged when using the approach and methods used in this study: (i) Sentinel2's optical sensors cannot penetrate clouds, leading to missing observations during cloudy seasons. In regions with frequent cloud cover, especially during the monsoon or rainy seasons, key phenological phases may be unobserved, reducing classification accuracy (Claverie et al. 2018). However, the integration of Sentinel 1 datasets allowed for more data availability (data filling). (ii) The SVM and RF models were trained in this study using datasets collected on FAW infestation on maize crops in Bangladesh, however planting schedules, management practices, environmental conditions (such as soil moisture and roughness) can differ substantially in other agroecological zones or with different crop species (Atzberger 2013), which would affect the spectral signatures and the generalizability of our methods to other crops and regions. (iii) In regions with many smallholder farmers, especially in Asia and Africa, where fields often exhibit heterogeneous planting patterns such as intercropping, data cleaning is especially critical during the initial stages of analysis.

The dataset did not include the most extreme soil moisture (<10% or >25%) or crop density (<50 or >300 plants m^{-2}) regimes. Changes in the environmental conditions, such as soil moisture, are expected to alter the reflectance (Darvishzadeh et al. 2009; Gao et al. 2022) therefore, the generalizability of the models under varying soil conditions needs further study.

6. Conclusions and recommendations

The approach used in this study to map FAW infestation in maize with Sentinel-1 and Sentinel-2 data shows strong potential for application in other regions. This study demonstrates that integrating Sentinel1 and Sentinel2 satellite imagery with machine learning techniques, specifically RF and SVM algorithms to effectively detect FAW infestations in maize fields. Compared to prior research that often relied on single-source data or single-model classification, this study presents a more comprehensive and adaptable framework. These innovations not only enhance detection performance but also contribute to the development of more scalable and operational pest monitoring systems. This approach demonstrates the added value of fusing Sentinel 1 and Sentinel2 for FAW detection. The findings indicate that these methods serve as reliable and accessible benchmarks for remote sensing-based pest detection, thereby supporting advancements in precision agriculture. However, its transferability may be affected by factors such as climatic variations, crop management practices, and pest population dynamics.

To improve its applicability, future research should validate the approach across diverse agricultural settings and refine models with region-specific calibration. Expanding its use to detect other crop pests could further enhance its impact on precision pest management. The integration of multi-sensor remote sensing with machine learning and vegetation indices offers a scalable and adaptable method for different agroecological zones. It is crucial for policymakers to make use of this information to deal with the pest infestation at a national level and, in that way, be able to provide the needed help in the most vulnerable areas before more damage is done. Future research should consider other factors such as the environment and the climate changes in the particular study and how that affects or supports the EO datasets.

Acknowledgment

The authors wish to express their sincere gratitude to the Department of Agricultural Extension (DAE) in Bangladesh for their invaluable assistance in collecting field observations and generously sharing the associated data. The fieldwork was supported by the USAID/Bangladesh-funded Fighting Fall Armyworm Project and the Feed the Future Integrated Pest Management Activity, with additional backing from the CGIAR initiatives: Transforming Agrifood Systems in South Asia (TAFSSA; https://www.cgiar.org/initiative/20-transforming-agrifood-systems-in-south-asia-tafssa/.) and Crop Health Initiatives (PHI; https://www.cgiar.org/initiative/crop-health/). We also gratefully acknowledge the funding contributions from the National Research Foundation (NRF) of South Africa and Nuffic to this project (Grant number: 140927). Finally, we extend our heartfelt thanks to the reviewers for their insightful and constructive comments, which have greatly improved the quality of this manuscript.

Disclosure statement

The authors declare that they have no known competing financial interests or personal relationships that could have appeared to influence the work reported in this paper.

No potential conflict of interest was reported by the author(s).

Funding

This work was supported by the National Research Foundation (NRF) of South Africa and Nuffic [140927].

ORCID

Tatenda Dzurume http://orcid.org/0000-0002-9536-4012
Roshanak Darvishzadeh http://orcid.org/0000-0001-7512-0574
Timothy Dube http://orcid.org/0000-0003-3456-8991
T.S Amjath Babu http://orcid.org/0000-0001-9902-7104
Mutasim Billah http://orcid.org/0009-0002-0910-3682
Mustafa Kamal http://orcid.org/0000-0003-0473-5322
Md. Harun-Or-Rashid http://orcid.org/0000-0001-8890-1396
Md. Mostafizur Rahman Shah http://orcid.org/0000-0003-3452-1966
Timothy J. Krupnik http://orcid.org/0000-0001-6973-0106

Andrew Nelson http://orcid.org/0000-0002-7249-3778

Data availability

The data that support the findings of this study are available from the corresponding author, [T.D], upon reasonable request.

CRediT

Tatenda Dzurume: Writing – review & editing, Writing – original draft, Visualization, Validation, Software, Resources, Methodology, Investigation, Funding acquisition, Formal analysis, Conceptualization. Roshanak Darvishzadeh: Writing – review & editing, Supervision, Resources, Methodology, Conceptualization. Timothy Dube: Writing –review & editing, Supervision, Resources, Conceptualization. T.S. Amjath Babu: Writing –review & editing. Mutasim Billah: Writing – review & editing. Syed Nurul Alam: Writing – review & editing. Mustafa Kamal: Writing –review & editing, Resources. Md. Harun-Or-Rashid: Writing – review & editing, Resources. Badal Chandra Biswas: Writing – review & editing. Md Ashraf Uddin: Writing – review & editing. Md Abdul Muyeed: Writing – review & editing. Md. Mostafizur Rahman Shah: Writing –review & editing. Timothy J. Krupnik: Writing – review & editing, Resources. Andrew Nelson: Writing – review & editing, Supervision, Resources, Project administration, Methodology, Conceptualization.

References

Abdullah, H., A. K. Skidmore, R. Darvishzadeh, and M. Heurich. 2019. "Sentinel-2 Accurately Maps Green-Attack Stage of European Spruce Bark Beetle (Ips Typographus, L.) Compared with Landsat-8." *Remote Sensing in Ecology and Conservation* 5 (1): 87–106. https://doi.org/10.1002/rse2.93.

Abro, Z., E. Kimathi, H. de Groote, T. Tefera, S. Sevgan, S. Niassy, M. Kassie, and R. N. Nagoshi. 2021. "Socioeconomic and Health Impacts of Fall Armyworm in Ethiopia." *PLOS ONE* 16 (11): e0257736. https://doi.org/10.1371/journal.pone.0257736.

Adan, M., H. E. Z. Tonnang, K. Greve, C. Borgemeister, and G. Goergen. 2023. "Use of Time Series Normalized Difference Vegetation Index (NDVI) to Monitor Fall Armyworm (Spodoptera Frugiperda) Damage on Maize Production Systems in Africa." *Geocarto International* 38 (1). https://doi.org/10.1080/10106049.2023.2186492.

Adelabu, S., O. Mutanga, and E. Adam. 2014. "Evaluating the Impact of Red-Edge Band from RapidEye Image for Classifying Insect Defoliation Levels." *ISPRS Journal of Photogrammetry & Remote Sensing* 95:34–41. https://doi.org/10.1016/j.isprsjprs.2014.05.013.

Adugna, T., W. Xu, and J. Fan. 2022. "Comparison of Random Forest and Support Vector Machine Classifiers for Regional Land Cover Mapping Using Coarse Resolution FY-3C Images." *Remote Sensing* 14 (3): 574. https://doi.org/10.3390/rs14030574.

Ainunnisa, I., and H. Haerani. 2023. "The Identification of Pests and Diseases of Rice Plants Using Sentinel-2 Satellite Imagery Data at the End of the Vegetative Stage." *IOP Conference Series Earth and Environmental Science* 1230 (1): 012148. https://doi.org/10.1088/1755-1315/1230/1/012148.

Ali, A. M., R. Darvishzadeh, and A. K. Skidmore. 2017. "Retrieval of Specific Leaf Area from Landsat-8 Surface Reflectance Data Using Statistical and Physical Models." *IEEE Journal of Selected Topics in Applied Earth Observations & Remote Sensing* 10 (8): 3529–3536. https://doi.org/10.1109/JSTARS.2017.2690623.

Attaluri, S., K. Gyeltshen, N. Sultana, and M. B. Hossain. 2022. *Fall Armyworm (FAW) Spodoptera frugiperda*. www.sac.org.bd.

Atzberger, C. 2013. "Advances in Remote Sensing of Agriculture: Context Description, Existing Operational Monitoring Systems and Major Information Needs." *Remote Sensing* 5 (2): 949–981. https://doi.org/10.3390/rs5020949.

Balla, A., P. Bagade, and N. Rawal. 2019. "Yield Losses in Maize (Zea Mays) Due to Fall Armyworm Infestation and Potential IoT-Based Interventions for Its Control." *Journal of Entomology and Zoology Studies* 7 (5): 920–927. http://www.entomoljournal.com.

Banks, S., L. White, A. Behnamian, Z. Chen, B. Montpetit, B. Brisco, J. Pasher, and J. Duffe. 2019. "Wetland Classification with Multi-Angle/Temporal SAR Using Random Forests." *Remote Sensing* 11 (6): 670. https://doi.org/10.3390/rs11060670.

Barnes, E. Clarke, T. Richards, S. Colaizzi, P. Haberland, J. Kostrzewski, M. Waller, P. Choi, C. Riley, E. Thompson. et al. 'Coincident detection of crop water stress, nitrogen status and canopy density using ground based multispectral data''. In Proceedings of the Fifth International Conference on Precision Agriculture, Bloomington, MN, USA, 16–19 July 2000.

Belgiu, M., and L. Drăgu. 2016. "Random Forest in Remote Sensing: A Review of Applications and Future Directions." In *ISPRS Journal of Photogrammetry and Remote Sensing*, 24–31. Vol. 114. Amsterdam, Netherlands: Elsevier B.V. https://doi.org/10.1016/j.isprsjprs.2016.01.011.

Bhattarai, R., P. Rahimzadeh-Bajgiran, A. Weiskittel, and D. A. MacLean. 2020. "Sentinel-2 Based Prediction of Spruce Budworm Defoliation Using Red-Edge Spectral Vegetation Indices." *Remote Sensing Letters* 11 (8): 777–786. https://doi.org/10.1080/2150704X.2020.1767824.

Bhattarai, R., P. Rahimzadeh-Bajgiran, A. Weiskittel, A. Meneghini, and D. A. MacLean. 2021. "Spruce Budworm Tree Host Species Distribution and Abundance Mapping Using Multi-Temporal Sentinel-1 and Sentinel-2 Satellite Imagery." *ISPRS Journal of Photogrammetry & Remote Sensing* 172:28–40. https://doi.org/10.1016/j.isprsjprs.2020.11.023.

Bouman, M. B. A., J. van Kasteren. 1990. "Ground-Based X-Band (3-Cm Wave) Radar Backscattering of Agricultural Crops." *II Wheat, Barley, and Oats; the Impact of Canopy Structure* 34 (2): 107–119. https://doi.org/10.1016/0034-4257(90)90102-R.

Breiman, L. 2001. "Random Forests." *Machine Learning* 45 (1): 5–32. https://doi.org/10.1023/A:1010933404324.

Breiman, L. 2001. "Random Forests." *Machine Learning* 45: 5–32.

Brouder, S. M., and J. J. Volenec. 2008. "Impact of Climate Change on Crop Nutrient and Water Use Efficiencies." *Physiologia Plantarum* 133 (4): 705–724. https://doi.org/10.1111/j.1399-3054.2008.01136.x.

Carvalho, M., A. J. Pinho, and S. Brás. 2025. "Resampling Approaches to Handle Class Imbalance: A Review from a Data Perspective." *Journal of Big Data* 12 (1). https://doi.org/10.1186/s40537-025-01119-4.

Chauhan, S., R. Darvishzadeh, Y. Lu, M. Boschetti, and A. Nelson. 2020. "Understanding Wheat Lodging Using Multi-Temporal Sentinel-1 and Sentinel-2 Data." *Remote Sensing of Environment* 243:243. https://doi.org/10.1016/j.rse.2020.111804.

Chauhan, S., R. Darvishzadeh, Y. Lu, D. Stroppiana, M. Boschetti, M. Pepe, and A. Nelson. 2019. "Wheat Lodging Assessment Using Multispectral UAV Data." *International Archives of the Photogrammetry, Remote Sensing and Spatial Information Sciences - ISPRS Archives* 42 (2/W13): 235–240. https://doi.org/10.5194/isprs-archives-XLII-2-W13-235-2019.

Chen J M. (1996). Evaluation of Vegetation Indices and a Modified Simple Ratio for Boreal Applications. Canadian Journal of Remote Sensing, 22(3), 229–242. 10.1080/07038992.1996.10855178

Chinwada, P. 2021. *Identification of Fall Armyworm and Confounding Pests in Maize Agroecosystems*: *An Illustrated Guide Identification of Fall Armyworm and Confounding Pests in Maize Agroecosystems*. http://extension.cropsciences.illinois.edu/fieldcrops/insects/black_cutworm/:.

Claverie, M., J. Ju, J. G. Masek, J. L. Dungan, E. F. Vermote, J. C. Roger, S. V. Skakun, and C. Justice. 2018. "The Harmonized Landsat and Sentinel-2 Surface Reflectance Data Set." *Remote Sensing of Environment* 219:145–161. https://doi.org/10.1016/j.rse.2018.09.002.

Cortes, C., V. Vapnik, and L. Saitta. 1995. “Support-Vector Networks Editor.” In *Machine Leaming*, Vol. 20. Boston, MA.: Kluwer Academic Publishers 273–297 doi:https://doi.org/10.1007/BF00994018.

Darvishzadeh, R., C. Atzberger, A. K. Skidmore, and A. A. Abkar. 2009. “Leaf Area Index Derivation from Hyperspectral Vegetation Indices and the Red Edge Position.” *International Journal of Remote Sensing* 30 (23): 6199–6218. https://doi.org/10.1080/01431160902842342.

Das, P., P. Rahimzadeh-Bajgiran, W. Livingston, C. D. McIntire, and A. Bergdahl. 2024. “Modeling Forest Canopy Structure and Developing a Stand Health Index Using Satellite Remote Sensing.” *Ecological Informatics* 84:84. https://doi.org/10.1016/j.ecoinf.2024.102864.

Daughtry, C. S., Walthall, C. L., Kim, M. S., Brown de Colstoun, E., & McMurtrey III, J. E. (1999). Estimating Corn Leaf Chlorophyll Concentration from Leaf and Canopy Reflectance. In REMOTE SENS. ENVIRON (Vol. 74).

Day, R., P. Abrahams, M. Bateman, T. Beale, V. Clottey, M. Cock, Y. Colmenarez, et al. 2017. “Fall Armyworm: Impacts and Implications for Africa.” *Outlooks on Pest Management* 28 (5): 196–201. https://doi.org/10.1564/v28_oct_02.

Della Bellver, F., B. Franch Gras, I. Moletto-Lobos, C. J. Guerrero Benavent, A. San Bautista Primo, C. Rubio, E. Vermote, and S. Saunier. 2024. “Pest Detection in Citrus Orchards Using Sentinel-2: A Case Study on Mealybug (Delottococcus aberiae) in Eastern Spain.” *Remote Sensing* 16 (23): 4362. https://doi.org/10.3390/rs16234362.

Dhau, I., T. Dube, and T. D. Mushore. 2021. “Examining the Prospects of Sentinel-2 Multispectral Data in Detecting and Mapping Maize Streak Virus Severity in Smallholder Ofcolaco Farms, South Africa.” *Geocarto International* 36 (16): 1873–1883. https://doi.org/10.1080/10106049.2019.1669724.

Dunn, O. 1964. “Multiple Comparisons Using Rank Sums.” *Technometrics* 6 (3): 241. https://doi.org/10.2307/1266041.

Durocher-Granger, L., G. M. Wu, E. A. Finch, A. Lowry, Y. T. Yeap, J. M. Bonnin, L. Offord, M. Kenis, and M. Dicke. 2024. “Preliminary Results on Effects of Planting Dates and Maize Growth Stages on Fall Armyworm Density and Parasitoid Occurrence in Zambia.” *CABI Agriculture and Bioscience* 5 (1). https://doi.org/10.1186/s43170-024-00258-7.

Dutta, A., R. Tyagi, A. Chattopadhyay, D. Chatterjee, A. Sarkar, B. Lall, and S. Sharma. 2024. “Early Detection of Wilt in Cajanus Cajan Using Satellite Hyperspectral Images: Development and Validation of Disease-Specific Spectral Index with Integrated Methodology.” *Computers and Electronics in Agriculture* 219:219. https://doi.org/10.1016/j.compag.2024.108784.

Dzurume, T., R. Darvishzadeh, T. Dube, T. S. A. Babu, M. Billah, S. N. Alam, M. Kamal, et al. 2025. “Detection of Fall Armyworm Infestation in Maize Fields During Vegetative Growth Stages Using Temporal Sentinel-2.” *International Journal of Applied Earth Observation and Geoinformation* 139:104516. https://doi.org/10.1016/j.jag.2025.104516.

Eitel, J. U. H., L. A. Vierling, M. E. Litvak, D. S. Long, U. Schulthess, A. A. Ager, D. J. Krofcheck, and L. Stoscheck. 2011. “Broadband, Red-Edge Information from Satellites Improves Early Stress Detection in a New Mexico Conifer Woodland.” *Remote Sensing of Environment* 115 (12): 3640–3646. https://doi.org/10.1016/j.rse.2011.09.002.

Eschen, R., T. Beale, J. M. Bonnin, K. L. Constantine, S. Duah, E. A. Finch, F. Makale, et al. 2021. “Towards Estimating the Economic Cost of Invasive Alien Species to African Crop and Livestock Production.” *CABI Agriculture and Bioscience* 2 (1). https://doi.org/10.1186/s43170-021-00052-9.

Feng, Z., L. Song, J. Duan, L. He, Y. Zhang, Y. Wei, and W. Feng. 2022. “Monitoring Wheat Powdery Mildew Based on Hyperspectral, Thermal Infrared, and RGB Image Data Fusion.” *Sensors* 22 (1): 31. https://doi.org/10.3390/s22010031.

Fernández, C. I., B. Leblon, A. Haddadi, K. Wang, and J. Wang. 2020. “Potato Late Blight Detection at the Leaf and Canopy Levels Based in the Red and Red-Edge Spectral Regions.” *Remote Sensing* 12 (8): 1292. https://doi.org/10.3390/RS12081292.

Fernández, F.G, and R.G Hoeft. 2009 Illinois Agronomy Handbook 91–112. “.”

Filho, F. H. I., J. B. de Bastos Pazini, A. D. de Medeiros, D. L. Rosalen, and P. T. Yamamoto. 2022. “Assessment of Injury by Four Major Pests in Soybean Plants Using Hyperspectral Proximal Imaging.” *Agronomy* 12 (7): 1516. https://doi.org/10.3390/agronomy12071516.

Francesconi, S., A. Harfouche, M. Maesano, and G. M. Balestra. 2021. "UAV-Based Thermal, RGB Imaging and Gene Expression Analysis Allowed Detection of Fusarium Head Blight and Gave New Insights into the Physiological Responses to the Disease in Durum Wheat." *Frontiers in Plant Science* 12:12. https://doi.org/10.3389/fpls.2021.628575.

Franke, J., and G. Menz. 2007. "Multi-Temporal Wheat Disease Detection by Multi-Spectral Remote Sensing." *Precision Agriculture* 8 (3): 161–172. https://doi.org/10.1007/s11119-007-9036-y.

Fu, H., H. Zhao, R. Song, Y. Yang, Z. Li, and S. Zhang. 2022. "Cotton Aphid Infestation Monitoring Using Sentinel-2 MSI Imagery Coupled with Derivative of Ratio Spectroscopy and Random Forest Algorithm." *Frontiers in Plant Science* 13. https://doi.org/10.3389/fpls.2022.1029529.

Furuya, D. E. G., L. Ma, M. M. Faita Pinheiro, F. D. Georges Gomes, W. N. Gonçalvez, J. M. Junior, D. de Castro Rodrigues, et al. 2021. "Prediction of Insect-Herbivory-Damage and Insect-Type Attack in Maize Plants Using Hyperspectral Data." *International Journal of Applied Earth Observation and Geoinformation* 105:102608. https://doi.org/10.1016/j.jag.2021.102608.

Galani, Y. J. H., C. Orfila, and Y. Y. Gong. 2022. "A Review of Micronutrient Deficiencies and Analysis of Maize Contribution to Nutrient Requirements of Women and Children in Eastern and Southern Africa." *Critical Reviews in Food Science and Nutrition* 62 (6): 1568–1591. https://doi.org/10.1080/10408398.2020.1844636.

Gao, L., R. Darvishzadeh, B. Somers, B. A. Johnson, Y. Wang, J. Verrelst, X. Wang, and C. Atzberger. 2022. "Hyperspectral Response of Agronomic Variables to Background Optical Variability: Results of a Numerical Experiment." *Agricultural and Forest Meteorology* 326:109178. https://doi.org/10.1016/j.agrformet.2022.109178.

Gitelson, A. A., A. Viña, V. Ciganda, D. C. Rundquist, and T. J. Arkebauer. 2005. "Remote Estimation of Canopy Chlorophyll Content in Crops." *Geophysical Research Letters* 32 (8): 1–4. https://doi.org/10.1029/2005GL022688.

Gitelson, A., and M. N. Merzlyak. 1994. "Spectral Reflectance Changes Associated with Autumn Senescence of Aesculus Hippocastanum L. and Acer Platanoides L. Leaves. Spectral Features and Relation to Chlorophyll Estimation." *Journal of Plant Physiology* 143 (3): 286–292. https://doi.org/10.1016/S0176-1617(11)81633-0.

Goyal, P., R. Sharda, M. Saini, and M. Siag. 2024. "A Deep Learning Approach for Early Detection of Drought Stress in Maize Using Proximal Scale Digital Images." *Neural Computing & Applications* 36 (4): 1899–1913. https://doi.org/10.1007/s00521-023-09219-z.

Greene, A. D., F. P. F. Reay-Jones, K. R. Kirk, B. K. Peoples, and J. K. Greene. 2021. "Spatial Associations of Key Lepidopteran Pests with Defoliation, NDVI, and Plant Height in Soybean." *Environmental Entomology* 50 (6): 1378–1392. https://doi.org/10.1093/ee/nvab098.

Guyon, I., J. Weston, and S. Barnhill. 2002. "Gene Selection for Cancer Classification Using Support Vector Machines." *Machine Learning* 46 (1–3): 389–422. https://doi.org/10.1023/A:1012487302797.

Haboudane, D., J. R. Miller, N. Tremblay, P. J. Zarco-Tejada, and L. Dextraze. 2002. "Integrated Narrow-Band Vegetation Indices for Prediction of Crop Chlorophyll Content for Application to Precision Agriculture." www.elsevier.com/locate/rse.

He, H., and E. A. Garcia. 2009. "Learning From Imbalanced Data." *IEEE Transactions on Knowledge and Data Engineering* 21 (9): 1263–1284. https://doi.org/10.1109/TKDE.2008.239.

Horler D N, Dockray M and Barber J. (1983). The red edge of plant leaf reflectance. International Journal of Remote Sensing, 4(2), 273–288. 10.1080/01431168308948546

Hoseny, M. M. E., H. F. Dahi, A. M. E. Shafei, and M. S. Yones. 2023. "Spectroradiometer and Thermal Imaging as Tools from Remote Sensing Used for Early Detection of Spiny Bollworm, Earias insulana (Boisd.) Infestation." *International Journal of Tropical Insect Science* 43 (1): 245–256. https://doi.org/10.1007/s42690-022-00917-0.

Ishengoma, F. S., I. A. Rai, and R. N. Said. 2021. "Identification of Maize Leaves Infected by Fall Armyworms Using UAV-Based Imagery and Convolutional Neural Networks." *Computers and Electronics in Agriculture* 184:184. https://doi.org/10.1016/j.compag.2021.106124.

Isip, M. F., R. T. Alberto, and A. R. Biagtan. 2020. "Exploring Vegetation Indices Adequate in Detecting Twister Disease of Onion Using Sentinel-2 Imagery." *Spatial Information Research* 28 (3): 369–375. https://doi.org/10.1007/s41324-019-00297-7.

Islam, M. R., and S. Hoshain. 2022. "A Brief Review on the Present Status, Problems and Prospects of Maize Production in Bangladesh." *Research in Agriculture Livestock and Fisheries* 9 (2): 89–96. https://doi.org/10.3329/ralf.v9i2.61613.

Jia, X., D. Yin, Y. Bai, X. Yu, Y. Song, M. Cheng, S. Liu, et al. 2023. "Monitoring Maize Leaf Spot Disease Using Multi-Source UAV Imagery." *Drones* 7 (11): 650. https://doi.org/10.3390/drones7110650.

Kara, S., B. Maden, B. S. Ercan, F. Sunar, T. Aysal, and O. Saglam. 2023. "Assessing the Impact of Beet Webworm Moths on Sunflower Fields Using Multitemporal Sentinel-2 Satellite Imagery and Vegetation Indices." *International Archives of the Photogrammetry, Remote Sensing and Spatial Information Sciences*, *XLVIII-M-1–2023*, 521–527. https://doi.org/10.5194/isprs-archives-xlviii-m-1-2023-521-2023.

Kassie, M., T. Wossen, H. De Groote, T. Tefera, S. Sevgan, and S. Balew. 2020. "Economic Impacts of Fall Armyworm and Its Management Strategies: Evidence from Southern Ethiopia." *European Review of Agricultural Economics* 47 (4): 1473–1501. https://doi.org/10.1093/erae/jbz048.

Kaushik, S. K., V. N. Mishra, M. Punia, P. Diwate, T. Sivasankar, and A. K. Soni. 2021. "Crop Health Assessment Using Sentinel-1 SAR Time Series Data in a Part of Central India." *Remote Sensing in Earth Systems Sciences* 4 (4): 217–234. https://doi.org/10.1007/s41976-021-00064-z.

Khatun, M. M., M. R. Ali, M. S. Hossain, M. M. Haque, M. A. Latif, R. W. Bell, and M. Mainuddin. 2024. "Fall Armyworm (S. Frugiperda) an Emerging Risk for the Expansion of Maize in the Coastal Zone of Bangladesh: A Survey of Farmers' Perception and Practices." *Journal of the Indian Society of Coastal Agricultural Research* 42 (1). https://doi.org/10.54894/jiscar.42.1.2024.145442.

Kruskal, W. H., and W. A. Wallis. 1952. "Use of Ranks in One-Criterion Variance Analysis." *Journal of the American Statistical Association* 47 (260): 583–621. https://doi.org/10.1080/01621459.1952.10483441.

Kumbula, S. T., P. Mafongoya, K. Y. Peerbhay, R. T. Lottering, and R. Ismail. 2019. "Using Sentinel-2 Multispectral Images to Map the Occurrence of the Cossid Moth (Coryphodema Tristis) in Eucalyptus Nitens Plantations of Mpumalanga, South Africa." *Remote Sensing* 11 (3): 278. https://doi.org/10.3390/rs11030278.

Kumela, T., J. Simiyu, B. Sisay, P. Likhayo, E. Mendesil, L. Gohole, and T. Tefera. 2019. "Farmers' Knowledge, Perceptions, and Management Practices of the New Invasive Pest, Fall Armyworm (Spodoptera Frugiperda) in Ethiopia and Kenya." *International Journal of Pest Management* 65 (1): 1–9. https://doi.org/10.1080/09670874.2017.1423129.

Lamsal, S., S. Sibi, and S. Yadav. 2020. "Fall Armyworm in South Asia: Threats and Management." *Asian Journal of Advances in Agricultural Research*: 21–34. https://doi.org/10.9734/ajaar/2020/v13i330106.

Lu, J., H. Qiu, Q. Zhang, Y. Lan, P. Wang, Y. Wu, J. Mo, W. Chen, H. Y. Niu, and Z. Wu. 2022. "Inversion of Chlorophyll Content Under the Stress of Leaf Mite for Jujube Based on Model PSO-ELM Method." *Frontiers in Plant Science* 13. https://doi.org/10.3389/fpls.2022.1009630.

Ma, Y., G. Jiang, J. Huang, Y. Shen, H. Guan, Y. Dong, J. Li, and C. Hu. 2024. "Evaluating the Ability of the Sentinel-1 Cross-Polarization Ratio to Detect Spring Maize Phenology Using Adaptive Dynamic Threshold." *Remote Sensing* 16 (5): 826. https://doi.org/10.3390/rs16050826.

Mahlein, A. K., U. Steiner, H. W. Dehne, and E. C. Oerke. 2010. "Spectral Signatures of Sugar Beet Leaves for the Detection and Differentiation of Diseases." *Precision Agriculture* 11 (4): 413–431. https://doi.org/10.1007/s11119-010-9180-7.

Mandal, D., V. Kumar, D. Ratha, S. Dey, A. Bhattacharya, J. M. Lopez-Sanchez, H. McNairn, and Y. S. Rao. 2020. "Dual Polarimetric Radar Vegetation Index for Crop Growth Monitoring Using Sentinel-1 SAR Data." *Remote Sensing of Environment* 247:247. https://doi.org/10.1016/j.rse.2020.111954.

Matova, P. M., C. N. Kamutando, C. Magorokosho, D. Kutywayo, F. Gutsa, and M. Labuschagne. 2020. "Fall-Armyworm Invasion, Control Practices and Resistance Breeding in Sub-Saharan Africa." *Crop Science* 60 (6): 2951–2970. https://doi.org/10.1002/csc2.20317.

Meng, R., Z. Lv, J. Yan, G. Chen, F. Zhao, L. Zeng, and B. Xu. 2020. "Development of Spectral Disease Indices for Southern Corn Rust Detection and Severity Classification." *Remote Sensing* 12 (19): 1–16. https://doi.org/10.3390/rs12193233.

Mohanty, S. P., D. P. Hughes, and M. Salathé. 2016. "Using Deep Learning for Image-Based Plant Disease Detection." *Frontiers in Plant Science* 7 (September). https://doi.org/10.3389/fpls.2016.01419.

Montezano, D. G., A. Specht, D. R. Sosa-Gómez, V. F. Roque-Specht, J. C. Sousa-Silva, S. V. Paula-Moraes, J. A. Peterson, and T. E. Hunt. 2018. "Host Plants of Spodoptera Frugiperda (Lepidoptera: Noctuidae) in the Americas." *African Entomology* 26 (2): 286–300. https://doi.org/10.4001/003.026.0286.

Mudereri, B. T., E. M. Abdel-Rahman, S. Ndlela, L. D. M. Makumbe, C. C. Nyanga, H. E. Z. Tonnang, and S. A. Mohamed. 2022. "Integrating the Strength of Multi-Date Sentinel-1 and-2 Datasets for Detecting Mango (Mangifera Indica L.) Orchards in a Semi-Arid Environment in Zimbabwe." *Sustainability* (Switzerland) 14 (10): 5741. https://doi.org/10.3390/su14105741.

Mutanga, O., and A. K. Skidmore. 2004. "Narrow Band Vegetation Indices Overcome the Saturation Problem in Biomass Estimation." *International Journal of Remote Sensing* 25 (19): 3999–4014. https://doi.org/10.1080/01431160310001654923.

Nwanze, J. A. C., R. B. Bob-Manuel, U. Zakka, and E. B. Kingsley-Umana. 2021. "Population Dynamics of Fall Army Worm [(Spodoptera frugiperda) J.E. Smith] (Lepidoptera: Nuctuidae) in Maize-Cassava Intercrop Using Pheromone Traps in Niger Delta Region." *Bulletin of the National Research Centre* 45 (1). https://doi.org/10.1186/s42269-021-00500-6.

Oumar, Z and Mutanga, O. "Integrating environmental variables and WorldView-2 image data to improve the prediction and mapping of Thaumastocoris peregrinus (bronze bug) damage in plantation forests." ISPRS Journal of Photogrammetry and Remote Sensing 87 (2014): 39–46.

Prabhakar, M., K. A. Gopinath, N. R. Kumar, M. Thirupathi, U. S. Sravan, G. S. Kumar, G. S. Siva, G. Meghalakshmi, and S. Vennila. 2022. "Detecting the Invasive Fall Armyworm Pest Incidence in Farm Fields of Southern India Using Sentinel-2A Satellite Data." *Geocarto International* 37 (13): 3801–3816. https://doi.org/10.1080/10106049.2020.1869330.

Prabhakar, M., Y. G. Prasad, S. Vennila, M. Thirupathi, G. Sreedevi, G. Ramachandra Rao, and B. Venkateswarlu. 2013. "Hyperspectral Indices for Assessing Damage by the Solenopsis Mealybug (Hemiptera: Pseudococcidae) in Cotton." *Computers and Electronics in Agriculture* 97:61–70. https://doi.org/10.1016/j.compag.2013.07.004.

Prasanna, B. M., J. E. Huesing, and V. M. Peschke. 2021. *Fall Armyworm in Asia: A Guide for Integrated Pest Management*. www.maize.org.

Ramos, A. P. M., F. D. G. Gomes, M. M. F. Pinheiro, D. E. G. Furuya, W. N. Gonçalvez, J. M. Junior, M. F. F. Michereff, et al. 2022. "Detecting the Attack of the Fall Armyworm (Spodoptera Frugiperda) in Cotton Plants with Machine Learning and Spectral Measurements." *Precision Agriculture* 23 (2): 470–491. https://doi.org/10.1007/s11119-021-09845-4.

Ribeiro, A. V., L. N. Lacerda, M. A. Windmuller-Campione, T. M. Cira, Z. P. D. Marston, T. M. Alves, E. W. Hodgson, I. V. MacRae, D. J. Mulla, and R. L. Koch. 2024. "Economic-Threshold-Based Classification of Soybean Aphid, Aphis Glycines, Infestations in Commercial Soybean Fields Using Sentinel-2 Satellite Data." *Crop Protection* 177:106557. https://doi.org/10.1016/j.cropro.2023.106557.

Rouse, J., W. Haas, R., H. Schell, and J. A. Deering. 1974. 'Monitoring vegetation systems in the Great Plains with ERTS. In Proceedings of the Third Earth Resources Technology Satellite-1 Symposium''. December 10–15; Greenbelt, MD. Washington (DC): NASA. pp. 309–317

Ruan, C., Y. Dong, W. Huang, L. Huang, H. Ye, H. Ma, A. Guo, and Y. Ren. 2021. "Prediction of Wheat Stripe Rust Occurrence with Time Series Sentinel-2 Images." *Agriculture (Switzerland)* 11 (11): 1079. https://doi.org/10.3390/agriculture11111079.

Sári-Barnácz, F. E., M. Zalai, S. Toepfer, G. Milics, D. Iványi, M. Tóthné Kun, J. Mészáros, M. Árvai, and J. Kiss. 2023. "Suitability of Satellite Imagery for Surveillance of Maize Ear Damage by Cotton Bollworm (Helicoverpa armigera) Larvae." *Remote Sensing* 15 (23): 5602. https://doi.org/10.3390/rs15235602.

Savary, S., L. Willocquet, S. J. Pethybridge, P. Esker, N. McRoberts, and A. Nelson. 2019. "The Global Burden of Pathogens and Pests on Major Food Crops." *Nature Ecology & Evolution* 3 (3): 430–439. https://doi.org/10.1038/s41559-018-0793-y.

Senay, S. D., P. G. Pardey, Y. Chai, L. Doughty, and R. Day. 2022. "Fall Armyworm from a Maize Multi-Peril Pest Risk Perspective." *Frontiers in Insect Science* 2. https://doi.org/10.3389/finsc.2022.971396.

Sisay, B., J. Simiyu, E. Mendesil, P. Likhayo, G. Ayalew, S. Mohamed, S. Subramanian, and T. Tefera. 2019. “Fall Armyworm, Spodoptera Frugiperda Infestations in East Africa: Assessment of Damage and Parasitism.” *Insects* 10 (7): 195. https://doi.org/10.3390/insects10070195.

Tabu, H. I., A. M. Kankolongo, A. K. Lubobo, and L. N. Kimuni. 2024. “Maize Yield and Fall Armyworm Damage Responses to Genotype and Sowing Date-Associated Variations in Weather Conditions.” *The European Journal of Agronomy* 161:127334. https://doi.org/10.1016/j.eja.2024.127334.

Tanyi, C. B., R. N. Nkongho, J. N. Okolle, A. S. Tening, and C. Ngosong. 2020. “Effect of Intercropping Beans with Maize and Botanical Extract on Fall Armyworm (Spodoptera frugiperda) Infestation.” *International Journal of Agronomy* 2020:1–7. https://doi.org/10.1155/2020/4618190.

Tao, W., X. Wang, J. H. Xue, W. Su, M. Zhang, D. Yin, D. Zhu, Z. Xie, and Y. Zhang. 2022. “Monitoring the Damage of Armyworm as a Pest in Summer Corn by Unmanned Aerial Vehicle Imaging.” *Pest Management Science* 78 (6): 2265–2276. https://doi.org/10.1002/ps.6852.

Toepfer, S., P. Fallet, J. Kajuga, D. Bazagwira, I. P. Mukundwa, M. Szalai, and T. C. J. Turlings. 2021. “Streamlining Leaf Damage Rating Scales for the Fall Armyworm on Maize.” *Journal of Pest Science* 94 (4): 1075–1089. https://doi.org/10.1007/s10340-021-01359-2.

Tussupov, J., M. Yessenova, G. Abdikerimova, A. Aimbetov, K. Baktybekov, G. Murzabekova, and U. Aitimova. 2024. “Analysis of Formal Concepts for Verification of Pests and Diseases of Crops Using Machine Learning Methods.” *IEEE Access* 12:19902–19910. https://doi.org/10.1109/ACCESS.2024.3361046.

Veloso, A., S. Mermoz, A. Bouvet, T. Le Toan, M. Planells, J. F. Dejoux, and E. Ceschia. 2017. “Understanding the Temporal Behavior of Crops Using Sentinel-1 and Sentinel-2-Like Data for Agricultural Applications.” *Remote Sensing of Environment* 199:415–426. https://doi.org/10.1016/j.rse.2017.07.015.

Xulu, S., N. Mbatha, K. Peerbhay, M. Gebreslasie, and N. Agjee. 2024. “Comparison of Different Spectral Indices to Differentiate the Impact of Insect Attack on Planted Forest Stands.” *Remote Sensing Applications: Society & Environment* 33:101087. https://doi.org/10.1016/j.rsase.2023.101087.

Zarco-Tejada, P. J., J. R. Miller, A. Morales, A. Berjón, and J. Agüera. 2004. “Hyperspectral Indices and Model Simulation for Chlorophyll Estimation in Open-Canopy Tree Crops.” *Remote Sensing of Environment* 90 (4): 463–476. https://doi.org/10.1016/j.rse.2004.01.017.

Zhang, F., and X. Yang. 2020. “Improving Land Cover Classification in an Urbanized Coastal Area by Random Forests: The Role of Variable Selection.” *Remote Sensing of Environment* 251:251. https://doi.org/10.1016/j.rse.2020.112105.

Zhang, J., Y. Huang, R. Pu, P. Gonzalez-Moreno, L. Yuan, K. Wu, and W. Huang. 2019. “Monitoring Plant Diseases and Pests Through Remote Sensing Technology: A Review.” In *Computers and Electronics in Agriculture*, Vol. 165. Elsevier B.V., Amsterdam, Netherlands. https://doi.org/10.1016/j.compag.2019.104943.

Zhang, J., Y. Huang, L. Yuan, G. Yang, L. Chen, and C. Zhao. 2016. “Using Satellite Multispectral Imagery for Damage Mapping of Armyworm (Spodoptera Frugiperda) in Maize at a Regional Scale.” *Pest Management Science* 72 (2): 335–348. https://doi.org/10.1002/ps.4003.

Zhang, X., Y. Wu, L. Wang, and R. Li 2016. “Variable Selection for Support Vector Machines in Moderately High dimensions’.” *Source: Journal of the Royal Statistical Society. Series B (statistical Methodology)* 78. https://www.jstor.org/stable/24775327.